Inhibition of Bacterial Adhesion to Biomaterials by Cranberry Derived Proanthocyanidins

Irwin Adam Eydelnant, B.Eng.

Department of Chemical Engineering
McGill University, Montreal

May 2008

A thesis submitted to McGill University in partial fulfillment of the requirements of the degree of Master of Engineering

© Irwin Adam Eydelnant, 2008

Library and Archives Canada

Published Heritage Branch

395 Wellington Street
Ottawa ON K1A 0N4
Canada

Bibliothèque et Archives Canada

Direction du Patrimoine de l'édition

395, rue Wellington
Ottawa ON K1A 0N4
Canada

Your file Votre référence
ISBN: 978-0-494-51457-3
Our file Notre référence
ISBN: 978-0-494-51457-3

NOTICE:
The author has granted a non-exclusive license allowing Library and Archives Canada to reproduce, publish, archive, preserve, conserve, communicate to the public by telecommunication or on the Internet, loan, distribute and sell theses worldwide, for commercial or non-commercial purposes, in microform, paper, electronic and/or any other formats.

The author retains copyright ownership and moral rights in this thesis. Neither the thesis nor substantial extracts from it may be printed or otherwise reproduced without the author's permission.

AVIS:
L'auteur a accordé une licence non exclusive permettant à la Bibliothèque et Archives Canada de reproduire, publier, archiver, sauvegarder, conserver, transmettre au public par télécommunication ou par l'Internet, prêter, distribuer et vendre des thèses partout dans le monde, à des fins commerciales ou autres, sur support microforme, papier, électronique et/ou autres formats.

L'auteur conserve la propriété du droit d'auteur et des droits moraux qui protège cette thèse. Ni la thèse ni des extraits substantiels de celle-ci ne doivent être imprimés ou autrement reproduits sans son autorisation.

In compliance with the Canadian Privacy Act some supporting forms may have been removed from this thesis.

While these forms may be included in the document page count, their removal does not represent any loss of content from the thesis.

Conformément à la loi canadienne sur la protection de la vie privée, quelques formulaires secondaires ont été enlevés de cette thèse.

Bien que ces formulaires aient inclus dans la pagination, il n'y aura aucun contenu manquant.

Canada

"There is a pleasure in the pathless woods,
There is a rapture on the lonely shore,
There is society, where none intrudes,
By the deep sea, and music in its roar:
I love not man the less, but Nature more."

- Lord Byron

Table of Contents

List of Figures

List of Tables

Acknowledgements

This past year has been an exceptional one in terms of the challenges and obstacles met and overcome. Without the help and support of many great people this would have been impossible, and I am most grateful to you all.

To begin with I would like to thank my supervisor, Dr. Nathalie Tufenkji. For her optimism, support, and patience throughout my research, and the opportunities she has provided for me along the way.

Then Dr. Lorrie Kirshenbaum, who instilled in me a passion for research over the course of my undergraduate studies, and has been a great mentor and friend.

The Biocolloids Research Group, Andrew Pelley, Felipe Castro, Charles Poitras, Ivan Quevedo, and Caroline Warne-Zoueki, for making 6050 that much better of a place to exist.

My friends Ilana Ben-Ari, for making me breakfast when research took over, Ed Swanson, for constantly challenging and providing new ideas, and George Bekiaris, for always being.

Then to my parents and family. My mother for believing nothing is impossible. My father for his humour and support. My brothers and sisters for feigning interest in my work even when they had no idea what I was talking about.

Finally without funding nothing would be possible and for this I'd like to thank the Cranberry Research Institute, Wisconsin Cranberry Board, Brace Center for Water Resources Management, NSERC, and CFI.

Abstract

Nosocomial, or hospital acquired, infections, are ubiquitous within the modern clinical setting leading to over $5 billion annually of related healthcare costs in North America. All indwelling devices are highly susceptible to bacterial colonization where physico-chemical interactions between bacteria and biomaterial surfaces have been implicated as determinant factors in the fate of the initial adhesion processes. It has been proposed that by exploiting interference strategies within this critical step of infection the ability to create 'non-infective' biomaterials may be developed.

This thesis demonstrates the effectivity of North American cranberry (*Vaccinium macrocarpon)* derived proanthocyanidins in preventing the adhesion of pathogenic bacteria to biomaterial surfaces. Specifically, using a model of catheter associated urinary tract infection, significant reductions in initial adhesion of uropathogenic *Escherichia coli* and *Enterococcus faecalis* to PVC and PTFE were observed. With the application of colloidal theory, a mechanism of steric interference was determined as responsible for these effects.

The evidence presented implicates PAC as a molecule of interest for the development of novel biomaterials with increased resistance to bacteria colonization.

Abstract

Les infections nosocomiales, ou les infections acquises en milieu hospitalier, sont omniprésentes dans le cadre des cliniques modernes, menant à des dépenses de plus de $5 milliards en coûts médicaux reliés en Amérique du Nord, et ce, annuellement. Tous les appareils prosthétiques internes sont hautement susceptibles aux colonisations bactériologiques où des interactions physico-chimiques entre bactéries et surfaces bio-composites sont impliquées comme facteurs déterminants dans le sort final du processus d'adhésion initial. Il a été proposé d'explorer des stratégies interférentes dans cette étape cruciale d'infection de façon à créer un bio-composite ne permettant pas le développement d'infection.

Cette thèse démontre l'efficacité de proanthocyanides (PAC) dérivés de la canneberge nord-américaine (Vaccinium macrocarpon) afin de prévenir l'adhésion de bactéries infectieuses aux surfaces bio-composite. Précisément, utilisant un modèle de cathéter associé aux infections à étendue urinaire, des réductions significatives dans l'adhérence initiale d'uropathogène tel Escherichia coli et Enterococcus faecalis à PVC et PTFE ont été observées. Avec l'application de la théorie colloïdale, un mécanisme d'intervention stérique fut établit comme responsable de ces effets.

La preuve présentée implique PAC comme une molécule d'intérêt pour le développement d'un bio-composite original avec une plus grande résistance à la colonisation bactériologique.

Chapter One
Introduction

1.1 Scope

Catheter associated urinary tract infections (CAUTI) account for the majority of nosocomial infections acquired in both hospitals and nursing homes [1]. These infections are associated with a significant increase in mortality and have a considerable economic impact [1]. The main etiology of CAUTI is the initial adhesion of pathogenic bacteria to the lumen or extra-luminal surface of the catheter leading to biofilm formation that is often resistant to aggressive antibiotic treatment [2, 3]. Researchers have been seeking novel methods of modifying catheter surfaces in order to prevent bacterial colonization and subsequent biofilm formation [2, 3].

Bacterial biofilm formation has also been implicated in the development of community acquired urinary tract infections (UTI) [4], with the consumption of cranberry juice being recommended by clinicians as an effective method to prevent reoccurrence [5]. Furthermore, various compounds, including fructose and proanthocyanidins (PAC), have been identified as active compounds within cranberry being effective in preventing bacterial adhesion to uroepithelial cells [6, 7].

To date no evidence within the literature exists suggesting the potential of cranberry (*Vaccinium macrocarpon*) derived PACs in the prevention of uropathogenic microorganism adhesion to biomaterial surfaces. It is the goal of this study to investigate naturally derived PACs as a novel means in the prevention and treatment of CAUTI by catheter surface modification directly conjugated to biomaterials and the physico-chemical and/or genetic mechanisms associated with the anti-adhesive properties of PAC. This research may be expanded further to the treatment of a wide array of medical instruments including but limited to intravenous catheters, stents, and other implanted devices.

1.2 Objectives

This thesis serves to fulfill multiple objectives. The specific objectives of the research are:

1. To examine whether cranberry derived PACs can prevent adhesion of both Gram-negative and Gram-positive bacteria to biomaterial surfaces; and,

2. To identify the key mechanisms controlling the inhibition of bacteria to biomaterial surfaces in the presence of PAC. It is of interest to understand whether the prevention of bacterial adhesion to biomaterials in the presence of cranberry-derived PAC is controlled by a physicochemical surface phenomenon or metabolic responses to PAC; and,

3. To evaluate the growth, viability, and metabolic response of selected bacteria to PAC exposure by monitoring protein expression.

Chapter Two

Background & Theory|

2.1 Nosocomial Infection & CAUTI

In 2002, the National Nosocomial Infections Surveillance (NNIS) system in the United States, identified approximately 1.7 million cases of nosocomial infection, or hospital acquired infection, that resulted in nearly 100,000 deaths. Catheter associated urinary tract infection (CAUTI) accounted for nearly one-third of these cases, leading to nearly 14,000 deaths [1].

An evaluation of CAUTI pathogenesis is essential in the design of preventative strategies against infection [3]. In nearly all instances of CAUTI the infective organism is derived from the patient's own colonic and perineal flora or from the hands of the health care worker during catheter insertion [2]. After one week a quarter of catheterized patients develop CAUTI at a rate of 3-10% per day, with incidence approaching 100% after thirty days [8]. These infections are often asymptomatic however are nonetheless treated with unnecessary antibiotic therapies that have lead to catheter associated infections being the largest reservoir of drug resistant pathogenic microorganisms. Ultimately CAUTI results

in increased patient mortality, frequently being a precursor to endocarditis, sepsis, and other infections, with increased direct care costs in the realm of $500-$1000 per patient [2].

Two-thirds of CAUTI incidents progress from extraluminal contamination, either directly during catheter insertion, or by perineal microbes ascending along the mucous film contiguous with the external catheter surface. The remaining infections occur intraluminally due to microbial reflux ascending from the drainage container or bacteria descending from the patient's bladder [2]. The leading infective microorganisms isolated from CAUTI catheters are *E. coli* and *E. faecalis* together accounting for over half of all infections (see *Figure 2.1*) [1].

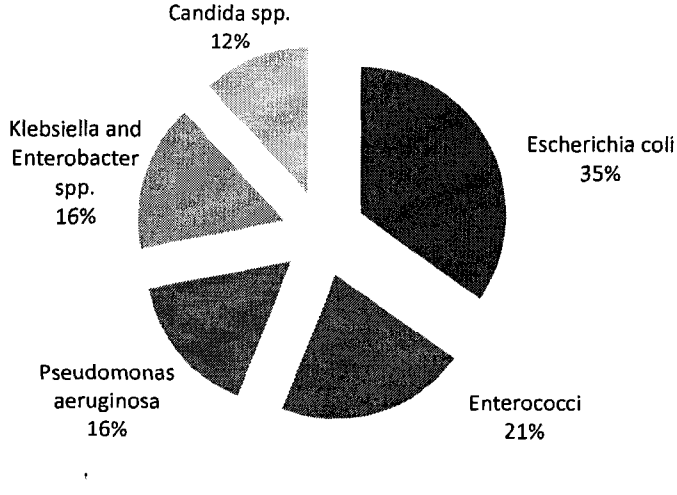

Figure 2.1: CAUTI pathogen statistics. *Proportion of pathogens isolated from infected indwelling urinary catheters in US acute care hospitals from 1990-92. Adapted from Klevens et al [1].*

Any implanted biomaterial is immediately susceptible to colonization by sessile microorganisms that eventually may develop into a biofilm [9]. Microbial organization into biofilm communities conveys survival advantages in the prevention of damage due to drying, shear forces, ultraviolet radiation, and antimicrobial agents [4]. These

properties consequently result in catheter removal and replacement as being the complete treatment of CAUTI. For the duration that the colonized catheter remains in place, biofilm-associated organisms can seed the urine with bacteria.

2.2 Biofilms

Initial observations of microbial biofilms were made by Van Leeuwenhoek in the seventeenth century in the plaque on his own teeth to which he ascribed the term "animalcules". It was not until 1978 that the definition of biofilm was formalized by Costerton explaining that the majority of bacteria grow in sessile biofilm communities adhered to surfaces that vary significantly from planktonic bacteria genetically and phenotypically [4]. Biofilms develop following the irreversible adhesion of microbes to exposed surfaces. The transition from planktonic to sessile life forms induces transcription of a variety of genes responsible for biofilm activity such as the production of extracellular polymers (EPS) and the incorporation of host proteins for the construction of a structural matrix [10]. Substrata for growth range in origins from inert, and abiotic surfaces to living tissues [4].

The preference of bacteria to form biofilm within high-shear environments has been described throughout the literature, with initial adhesion being observed at Reynold's numbers greater than 5000 [11]. Further the viscoelastic biofilm structures zunder these conditions are generally of higher tensile strength than biofilm grown under low shear. Localized detachment commences immediately with the initial adhesion of pioneer organisms. Detachment of sections of biofilm may occur due to failures within the bulk structure of the biofilm, whether that be weakening of the linking film, cohesive failure in the conditioning film, or interfacial rupture. Biofilm bacteria exhibit significantly different growth kinetics and antimicrobial responses due to physical limitations in the diffusion of oxygen and nutrient concentration, eventually leading to a 'steady-state' biofilm thickness where growth and attachment rates are matched by detachments rates [4]. The formation of biofilm in aqueous environments is considered a highly structured process as depicted in *Figure 2.2.*

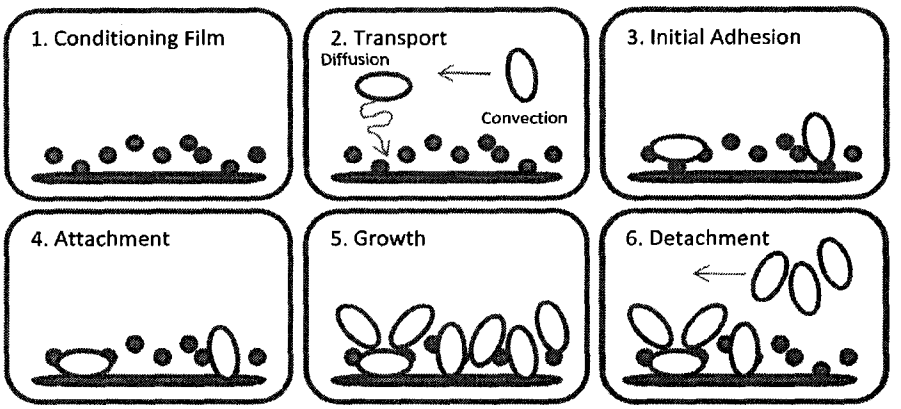

Figure 2.2: Development of microbial biofilm. *(1) A conditioning film of adsorbed organic matter is formed on the surface prior to the initial attachment, (2) Microorganisms are transported to the surface through classical transport phenomena including diffusion, convection, sedimentation, and active movement, (3) Initial non-specific adhesion occurs, (4) Attachment to the surface is enhanced by the production of EPS and unfolding of cell surface structures, (5) Growth of attached microbes occurs with increased EPS secretion, (6) Detachment of biofilm components occurs due to fluctuations in fluid shear forces and other mechanisms. Adapted from Gottenbos et al. [12]*

2.3 Prevention of Biofilm Formation

Originally the general belief was that inhibition of growth should be pursued in the prevention of biofilm formation. Designs implemented have included antibiotic slow-release materials and silver impregnated catheters designed to inactivate microbes on contact, however these approaches hold the risk of developing resistant strains [13] and have limited value for long-term use.

Today a significant faction of researchers hypothesize that the ideal method of blocking biofilm formation is preventing initial microbial adhesion. This process is mediated by specific interactions between cell surface structures and specific molecular groups on the substratum surface, or by non-specific interaction forces including Lifshitz-van der Waals forces, electrostatic forces, acid-base interaction [12, 14, 15]. Specific interactions differ from non-specific interactions in that they are essentially non-specific forces acting on highly localized areas at distances smaller than 5 nm. Non-specific interactions act over a longer range and originate from the entire body of the interacting surface.

Organisms will be attracted or repelled upon approach to a surface depending on the combination of non-specific interaction forces. Lifshitz-van der Waals forces generally promote bacterial adhesion, while electrostatic forces may be either attractive or repulsive. The negative charge carried by most microorganisms leads to repulsion upon approach to negatively charged substratum. By potentially controlling the charge and hydrophobic properties of surfaces, biofilm progression may be avoided or controlled [12].

Techniques such as ultrasound [16] and the application of low voltage electric fields at low current density [17] have been applied in the disruption of initial adhesion processes. Enzymatic attacks have been used in the destruction of EPS, with the intention of polymer dissipation obstructing the formation of biofilm ultrastructure [18]. As well early biofilm detection has been advocated as a valuable target in prevention as young biofilms are more susceptible to antimicrobial and chemical treatments than mature biofilms.

2.4 Cranberry Juice and Proanthocyanidins

Medical applications of the North American Cranberry (*Vaccinium macrocarpon)* were first documented in the 17^{th} century in the treatment and relief of blood disorders, stomach ailments, liver problems, vomiting, loss of appetite, scurvy, and cancer. Early Native Americans used whole dried fruit in the preparation of wound dressings in order to avoid infection. However the effects of cranberry dominated in their ability to provide relief from urinary tract infection (UTI). Original scientific beliefs were that cranberry consumption resulted in the acidification of urine and thereby prevented bacterial infection of the bladder, kidneys, and uroepithelium.

Though long recommended by physicians as a prophylactic treatment of UTI, it was not until the work of Sobota in 1984 that any basic research was performed documenting the effects of cranberry juice against uropathogens *in vitro*. Later Zafriri et al. identified two

pH independent anti-inhibitory mechanisms for the origins of these effects, fructose against the adhesion of Type 1 fimbriated *E. coli* and a non-dialyzable material (NDM) fraction against P-fimbriated *E. coli* to bladder cells. These effects were only pronounced upon the preincubation of bacteria in urine supplemented with the NDM fraction, leading to the hypothesis that the *in vivo* action of cranberry juice was occurring within the gut, the large reservoir of uropathogens. Mechanisms have also been suggested where cranberry extracts modify the production of Tamm-Horsfall glycoprotein, present in urine, that are known to provide anti-adherence effects against Type 1 *E. coli* to human kidney cells [19].

Changes in morphology and adhesion phenomena in bacteria exposed to cranberry juice and extract have also been documented. With the addition of cranberry juice to growth media loss of P-fimbriae [20], reduction of bacterial adhesion to mammalian cells [7, 20], and a reduction in surface adhesive force (measured by Atomic Force Microscopy) [21], have been reported. Ahuja demonstrated a transition from the typical short rounded rod shape of E. coli to extended rods (*Figure 2.3*). Camesano has observed the opposite effect, in a different strain, of E. coli observing a transition of cells from bacilli to cocci. As well, a change in Gram staining of these bacteria potentially due to changes within the peptidoglycan layer and lipopolysaccharides of the cells was demonstrated in the presence of cranberry juice.

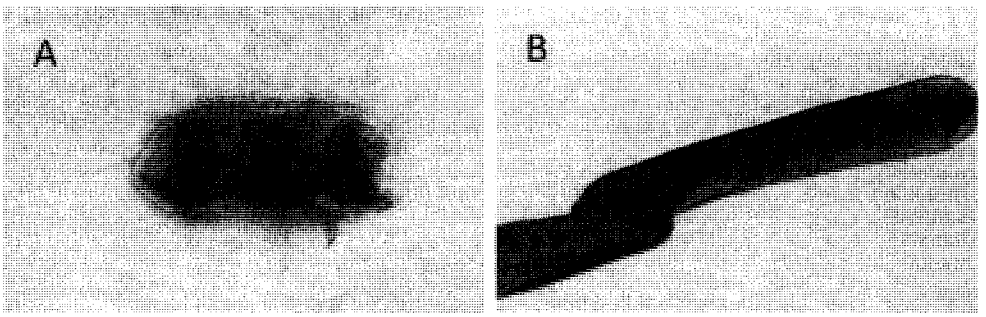

Figure 2.3: Effects of cranberry juice on bacteria morphology. *Electron micrographs of (A) E. coli JR1 cultured on colonizing factor antigen agar with fimbriae visible along the surface (CFA)*

and (B) Extended rod morphology of E. coli JR1 cultured on CFA supplemented with cranberry juice without visible fimbriae [20]

There have been limited numbers of relevant clinical studies fortifying the position of cranberry juice as an effective prophylactic and treatment for UTI. A systematic review of seven past clinicial trials was performed by Jepson et al. leading to the conclusion that evidence exists demonstrating that cranberry juice may decrease the risk of symptomatic UTIs over a 12 month period in women, though effectivity in other groups such as children and elderly men remained unknown [5]. There is evidence that consumption of dry cranberry fruit may also elucidate anti-adhesive activity in human urine [22].

Howell et al. were the first to demonstrate that proanthocyanidins (PACs) from the non-dialysable material (NDM) fraction of cranberry extract were responsible for inhibition of P-fimbriae adhesion and implicate PAC as the active compound in cranberry preventing uropathogen adhesion to uroepithelial cells [23]. Proanthocyanidins are composed of flavanol oligomers units, a polymer of flavan-3-ols. Past evidence has described the ability of proanthocyanidins (from sorghum) to specifically bind and precipitate proteins, with particular affinity for large proline rich macromolecules [24]. PACs derived from cranberry are particularly unique due to the A-type linkages between flavanol units as compared with the B-type linkages present in other foods such as grapes and chocolate [25]. Only these A-type PACs seem to have the ability to prevent bacterial adhesion to cellular surfaces. As well biochemical studies have revealed that cranberry components cause the compression of surface fimbriae, while also causing bacteria to change from rods to spheres, and preventing indole molecule quorum sensing [26]. Cranberries naturally contain approximately 0.5% phenolic compounds including PACs, therefore these molecules must be isolated and concentrated to observe increased effects [27]. Evidence exists demonstrating that bioactivity is associated with epicatechin units having DP 3 to 5 with at least one A-type linkage [28].

A recently published pilot study demonstrated the effectivity of cranberry extract supplement in the prevention of recurring female UTI [27]. 12 women diagnosed with chronic recurrent UTI were given 200 mg of cranberry extract twice daily containing 30% phenolic content, including PAC. Over long-term observation, these women who

had experienced more than 6 UTI events over the past 12 months, did not exhibit symptoms during treatment for up to two years. Further to lend to the possibility that PACs are responsible for the anti-adhesive properties of cranberry consumption, a study by Ohnishi et al. revealed that 5% of total ingested anthocyanidins were excreted through urine [29]. It is their hypothesis that the other compounds within cranberry potentially assist in absorption and secretion of anthocyanidins over those in other food products, though this has not been verified.

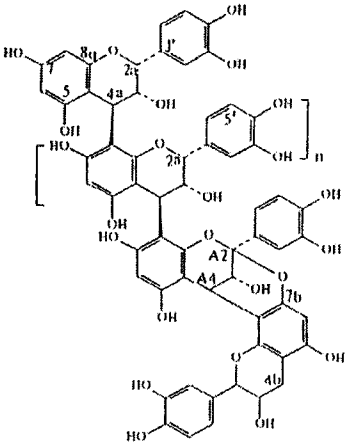

Figure 2.4: Chemical structure of PAC. *The compound consists of epicatechin subunits linked through A and B type linkages. Adapted from Foo et al.[6].*

2.5 Bacteria Surface Properties

Bacteria surfaces are characterized by structural and chemical heterogeneities featuring appendages such fibrils and fimbriae that extend into the surround media. The majority of bacteria in aqueous electrolyte exhibit a net negative electrostatic surface charge attributed to ionized phosphoryl and carboxyl groups of the outer cell envelope macromolecule constituents [30]. Lipopolysaccharides (LPS) and proteins on the surface of Gram-negative bacteria form charged surfaces that are stabilized by cation binding [31]. The chemical composition and configuration of these surface structures strongly affects bacteria surface charge, hydrophobicity, and consequently adhesion to surfaces

[32]. With respect to bacterial adhesion to abiotic surfaces, expression of fimbriae and autotransporter proteins has been demonstrated to be of significant interest.

2.5.1 Fimbriae

Bacterial fimbriae are the most frequent means by which *E. coli* adhere to uroepithelial cells, particularily Type 1-fimbriae (coded for by *fimH*) that adhere specifically to mannose receptors [33], and P-fimbriae (coded for by *pap*) that adhere to disaccharide alpha-D-Gal(1-4)-beta-D-Gal receptors. These receptors have been strongly implicated in potentiating bacterial adhesion and survival within the urinary tract and thereby leading to cystitis and pyelonephritis.

2.5.2 Autotransporter Proteins

Antigen 43 (Ag43) is a self-recognizing surface adhesion molecule that is expressed on the surface of most *Escherichia coli* strains. Increased expression of the autotransporter gene Ag43 causes aggregation of cells and enhances biofilm formation [34, 35], while mutations of the *flu* gene encoding for Ag43 generally results in cells with limited biofilm forming abilities [36]. This outer membrane protein occurs in most *E. coli* strains and not surprisingly is present in many enteropathogenic and uropathogenic strains with often duplex or multiple copies of the gene, particularily in enteropathogenic and enterohaemorrhagic strains [37].

2.6 Theoretical Models of Bacteria-Surface Interaction

Adhesion of bacteria to surfaces is highly dependent upon surface properties inherent to both the bacteria and the substrate. Correlations of bacterial adhesion have been attributed to hydrophobicity, zeta-potential, motility, and the production of extracellular substances including polysaccharides, proteins, and biosurfactants. Substrate properties of relevance include hydrophobicity and zeta potential. The sum of these properties have been modeled with the extended-DLVO (Derjaguin, Landau, Verwey, Overbeek) theory that includes Lifshitz-Van der Waals, electrostatic, and short-range acid-base interaction energies between bacteria and surfaces as a function of their separation distance. The

effects of surface grafted polymers are combined with these interactions through the development of the Alexander de Gennes equation providing theoretical models for adhesion processes. The subsequent text discusses the development of these equations.

2.6.1 van der Waals Forces

London-van der Waals forces are general attractive interactions between neutral atoms originally proposed by van der Waals in 1873. These interactions decay steeply for molecules and atoms as a function of increasing distance (l) as l^{-6}. In the classical, or microscopic, approach presented by Hamaker for interactions of macroscopic (i.e., two semi-infinite parallel plates) these decay rates are on the order of l^{-2} at distances shorter than 10 nm, and l^{-3} for greater distances due to retardation. Effects of retardation are incurred due to the electromagnetic nature of dispersion forces, thereby decreasing attractive interactions [38, 39]. The Gregory equation for retarded van der Waals interactions for sphere-plate geometries can be used in describing van der Waals interactions between bacteria and flat surfaces considering the assumption that h << a_p [40]:

$$\Delta G^{LW}(h) = -\frac{Aa_p}{6h}\left[1 - \frac{bh}{\lambda}\ln\left(1 + \frac{\lambda}{bh}\right)\right] \qquad \textit{Eq. 2.1}$$

where ΔG^{LW} is the van der Waals interaction potential energy, A is the Hamaker constant (as discussed in Section 2.6.3), a_p is the particle radius, h is the separation distance, b is the Gregory constant (b = 5.32), and λ the characteristic wavelength of the interaction ($\lambda \approx$ 100nm). The Czarnecki equation is another expression of van der Waals interactions for sphere-plate geometries and has been demonstrated as being minimally affected by substrate surface roughness [39].

2.6.2 Electrostatic Interactions

Any charged particle or substrate in electrolyte develops an electrical double layer (EDL) at its surface. This orientation of ions develops as an equal number of oppositely charged counterions surround the surface in order to balance the charge. Together the surface

charge and the surrounding ions compose the EDL. As charged particles or surfaces approach one another, their EDLs begin to interact then overlap [39]. When the particles bear a similar charge, repulsion is experienced, opposing attractive van der Waals forces. These charge effects are described by Hogg for sphere-plate geometries as [41]:

$$\Delta G^{EL}(h) = \frac{2\pi a_p n_\infty kT}{\kappa^2}(\phi_1^2 + \phi_2^2)\left[\frac{2\phi_1\phi_2}{\phi_1^2+\phi_2^2} ln\left(\frac{1+e^{-\kappa h}}{1-e^{-\kappa h}}\right) - \ln\left(1 - e^{-2\kappa h}\right)\right] \qquad Eq.\ 2.2$$

where a_p is the particle radius, n_∞ is the bulk number density of ions, κ is the Debye-Huckel reciprocal length, Φ_1 and Φ_2 are the reduced potentials of the particle and substrate surfaces respectively, and h is the separation distance. The bulk ion density (n_α) describes the number of ions in a given volume of electrolyte, and is derived from the ion concentration (C_s) and Avogadro's number (N_A):

$$n_\infty[\frac{ions}{m^3}] = 1000 N_A C_s \qquad Eq.\ 2.3$$

The reduced potential (Φ_i) is derived from the electrical surface potential (φ_i) that is estimated as being equivalent to the zeta-potential:

$$\Phi_i = \frac{ze\varphi_i}{kT} \qquad Eq.\ 2.4$$

where z is the electrolyte valence, e is the electron charge (4.4×10^{-10} e.s.u.), k is the Boltzmann constant, and T is the absolute temperature.

Electrokinetic techniques are used to measure zeta potential, however these analyses do not result in a true measure of surface charge, rather they approximate the potential at the mobile shear plane of the EDL. Streaming potential is used in the measure of zeta-potential at a flat surface and is determined by flowing a solution across the surface thereby creating a potential difference at each end. If the EDL is much thinner than the height or radius of the chamber the streaming current is readily determined using

Poiseuille's equations for laminar flow and the Poisson equation for the solution charge density. Electrophoretic mobility is commonly used in the determination of zeta-potential for particles. In the case that the particles that are large compared to the EDL, the Smoluchowski equation is used:

$$U = \frac{\epsilon\zeta}{\mu} \qquad \textit{Eq. 2.5}$$

where U is the electrophoretic mobility ($\mu ms^{-1}/Vcm^{-1}$), ε is the permittivity of the liquid medium (for water, $\varepsilon \approx 80$), ζ is the zeta-potential (mV), and μ is the fluid viscosity. For very small particles where $\kappa a << 1$, the Huckel equation is implemented. The inverse Debye-Huckel length (κ) refers to the thickness of the diffuse EDL and is dependent on both the concentration and type of electrolyte present (*Table 2.1*):

$$\kappa = \sqrt{\frac{e^2 \sum n_i z_i^2}{\varepsilon kT}} \qquad \textit{Eq. 2.6}$$

where e, z, ε, k, and T, have been previously defined, and n_i is the number of ions of species i.

Table 2.1 Debye length values in different electrolytes. *The Debye length as a function of electrolyte type (1-1, 1-2, and 2-2) and concentration. Adapted from van Oss [38].*

Solution	***1/κ (nm)***
H_2O	1000
10^{-5}M NaCl	100
10^{-3}M NaCl	10
10^{-1}M NaCl	1
10^{-5}M Na_2SO_4	56
10^{-3}M Na_2SO_4	5.6
10^{-1}M Na_2SO_4	0.56
10^{-5}M $MgSO_4$	48
10^{-3}M $MgSO_4$	4.8
10^{-1}M $MgSO_4$	0.48

2.6.3 *Surface Free Energy*

Surface free energy (γ) is defined as the work required for a unit increase in the surface area of matter. This surface free energy derives from the existence of 'unbound' molecules on the material surface, and is reduced through interactions with surrounding materials. In a bulk vapour phase this energy is termed 'surface energy' and 'surface tension', for condensed solid and liquid phases respectively. At condensed phase interfaces ($\gamma_{liquid\text{-}liquid}$ - γ_{ll}, $\gamma_{solid\text{-}solid}$ - γ_{ss}, $\gamma_{solid\text{-}liquid}$ - γ_{sl}) this energy is termed 'interfacial energy' [38].

In the evaluation of surface energies the thermodynamic approach inputs the contact angle between a liquid and the polymer or bacterial lawn surface, and relates this value to their respective surface free energies as described according to Thomas Young's relationship published in 1805 and known today as 'Young's equation':

$$\gamma_{lv}\cos\theta = \gamma_{sv} - \gamma_{sl} \qquad \textit{Eq. 2.7}$$

where l is the liquid, v is the surrounding vapour, and s is the solid surface, whether biomaterial or bacteria lawn.

In the solution of Young's equation, total surface free energy is treated as a sum of a Lifshitz-van der Waals (γ^{LW}) and an acid-base component (γ^{AB}) as first proposed by Fowkes. The acid-base component is then further expressed as a function of an electron donor (γ^-) and electron acceptor (γ^+) parameter.

$$\gamma^T = \gamma^{LW} + \gamma^{AB} = \gamma^{LW} + \gamma^+ + \gamma^- \qquad \textit{Eq. 2.8}$$

Combining Fowke's equation with Young's equation results in the following form:

$$cos\theta = -1 + \frac{2\sqrt{\gamma_{sv}^{LW}\gamma_{lv}^{LW}}}{\gamma_{lv}^{T}} + \frac{2\sqrt{\gamma_{sv}^{+}\gamma_{lv}^{-}}}{\gamma_{lv}^{T}} + \frac{2\sqrt{\gamma_{sv}^{-}\gamma_{lv}^{+}}}{\gamma_{lv}^{T}} \qquad \textit{Eq. 2.9}$$

In the absence of polar interactions, as is the case for most hydrocarbons (ie – diiodomethane), the Lifshitz-van der Waals component of free energy, γ_{sv}^{LW} is calculated directly from contact angle data using:

$$cos\theta = -1 + \frac{2\sqrt{\gamma_{sv}^{LW}\gamma_{lv}^{LW}}}{\gamma_{lv}^{T}} \qquad Eq.\ 2.10$$

Knowledge of the Lifshitz-van der Waals free energy component allows for the calculation of the Hamaker constant required for the calculation of van der Waals interaction forces according to:

$$\gamma_{ii}^{LW} = \frac{A_{ii}}{24\pi l_o^2} \qquad Eq.\ 2.11$$

where A_{ii} is the Hamaker constant and l_o is the minimum separation distance between the bacteria cell surface and the substratum (l_o = 0.157 nm [38]). The remaining surface energy parameters ($\gamma_{sv}^{+}, \gamma_{sv}^{-}$) of the acid-base component are calculated by resolving the system of two non-linear equations derived from contact angles measured using two additional polar liquids (ie – water and formamide). The acid-base component is calculated as follows:

$$\gamma_{sv}^{AB} = 2\sqrt{\gamma_{sv}^{+}\gamma_{sv}^{-}} \qquad Eq.\ 2.12$$

The Lifshitz-van der Waals and acid-base free energies of adhesion ($\Delta G_{slb}^{LW}, \Delta G_{slb}^{AB}$; where *s* is the substrate, *l* is the suspension media, and *b* is the bacteria) are calculated according to:

$$\Delta G_{slb}^{LW} = -2\left(\sqrt{\gamma_{bv}^{LW}} - \sqrt{\gamma_{lv}^{LW}}\right)\left(\sqrt{\gamma_{sv}^{LW}} - \sqrt{\gamma_{lv}^{LW}}\right) \qquad Eq.\ 2.13$$

$$\Delta G_{slb}^{AB} = 2\left[\left(\sqrt{\gamma_{bv}^{+}} - \sqrt{\gamma_{sv}^{+}}\right)\left(\sqrt{\gamma_{bv}^{-}} - \sqrt{\gamma_{sv}^{-}}\right) - \left(\sqrt{\gamma_{bv}^{+}} - \sqrt{\gamma_{lv}^{+}}\right)\left(\sqrt{\gamma_{bv}^{-}} - \sqrt{\gamma_{lv}^{-}}\right) - \left(\sqrt{\gamma_{sv}^{+}} - \sqrt{\gamma_{lv}^{+}}\right)\left(\sqrt{\gamma_{sv}^{-}} - \sqrt{\gamma_{lv}^{-}}\right)\right] \quad \textit{Eq. 2.14}$$

The total energy is the sum of these two components, with a negative value being indicative of thermodynamically favourable conditions and a positive value indicating thermodynamically unfavourable conditions:

$$\Delta G_{slb} = \Delta G_{slb}^{LW} + \Delta G_{slb}^{AB} \quad \textit{Eq. 2.15}$$

2.6.4 *Extended DLVO*

The total interaction energy upon approach of bacterial cell surfaces to biomaterial substrata was assessed within the context of extended DLVO theory for colloidal stability, assuming sphere-plate geometry. The theory requires the summation of the previously introduced interaction forces, van der Waals (*Eq. 2.1*) and electrostatic (*Eq. 2.2*), with a third accounting for acid-base interactions (*Eq. 2.14*). For sphere-plane geometry the equation describing acid-base interactions is [42]:

$$\Delta G^{AB}(h) = 2\Delta G_{slb}^{AB}\pi a_p \lambda \exp\left(\frac{l_o - h}{\lambda}\right) \quad \textit{Eq. 2.16}$$

where ΔG_{slb}^{AB} was determined in Equation 2.14, λ is the correlation length of molecules in liquid media ($\lambda \approx 0.6$ nm for hydrophilic bacteria, $\theta_{water} < 60°$, $\lambda \approx 13$ nm for hydrophobic bacteria, $\theta_{water} > 60°$) and l_o being previously defined in the determination of the Hamaker constant [42].

2.6.5 *Steric Interactions*

The adsorption of polymer layers onto colloidal surfaces may significantly impact deposition. *Bridging* is a phenomenon that occurs when low concentrations of the adsorbed polymer cover the particle/substrate surfaces leading to aggregation or

increased adhesion. However as the polymer concentration is increased an effect known as *steric stabilization* is generally observed. Due to the adsorbed layers, surfaces are maintained at sufficient distance from one another thereby preventing attractive van der Waals interactions, leading to an inhibition of adhesion [39].

Steric interactions between two parallel flat plates with grafted polymer layers in a good solvent are readily described by the Alexander-de Gennes equation [43]:

$$\frac{F(h)}{A} = \left(\frac{kT}{s^3}\right)\left[\left(\frac{2L}{h}\right)^{\frac{9}{4}} - \left(\frac{h}{2L}\right)^{\frac{3}{4}}\right] \qquad \textit{Eq. 2.17}$$

where h is the separation distance between spheres, F/A is the force per unit area, L is the polymer thickness, and s is the distance between polymer chains. This equation assumes that the polymer attached to the surface is linear, flexible, and neutral in good solvent with $h < 2L$. It can be modified for sphere-sphere interactions using the Derjaguin approximation [42]:

$$F(h) = \frac{2\pi(R_1R_2)}{R_1 + R_2}\int_h^\infty \frac{F(h)}{A}dh \qquad \textit{Eq. 2.18}$$

where R_1 and R_2 are the respective radii of the interacting spheres. Energy may be approximated for sphere-plate interactions by allowing the radius of one sphere to approach infinity then integrating the force over the separation distance. For systems with both surfaces coated with polymer:

$$E(h) = -2\pi R_1\left(\frac{kT}{s^3}\right)\int_\infty^h \left\{\frac{8L}{5}\left[\left(\frac{2L}{h}\right)^{\frac{5}{4}} - 1\right] + \frac{8L}{7}\left[\left(\frac{h}{2L}\right)^{\frac{7}{4}} - 1\right]\right\}dh \qquad \textit{Eq. 2.19}$$

For systems with a single polymer grafted surface a factor of 2 is removed preceding each L term:

$$E(h) = -2\pi R_1\left(\frac{kT}{s^3}\right)\int_h^\infty \left\{\frac{4L}{5}\left[\left(\frac{L}{h}\right)^{\frac{5}{4}} - 1\right] + \frac{4L}{7}\left[\left(\frac{h}{L}\right)^{\frac{7}{4}} - 1\right]\right\} dh \qquad \textit{Eq. 2.20}$$

When steric interactions are combined with xDLVO theory, electrostatic interactions are excluded as the grafted polymer is considered to have significantly modified the actual surface charge and surrounding EDL.

Typically AFM measurements are performed on the polymer grafted surface in order to yield force/distance measurements, which may then be fit with the modified Alexander-de Gennes equation yielding values for polymer thickness, L, and spacing, s. In this work, we implement a novel technique of calculating these values thereby yielding force profiles for inclusion in xDLVO calculations.

2.7 Hydrodynamics

Indwelling urinary catheters are tubular in design, however due to their relatively large radii of (in terms of mm) in comparison to the radii of bacteria (in terms of μm), parallel plate flow (PPF) systems are considered representative and are commonly used in modeling flow through catheters. Flow streamlines in the PPF system are parallel to the surface of interest. In order for bacteria to adhere they are required to exit the streamline either due to gravity, diffusion, interception, or inherent bacterial motility.

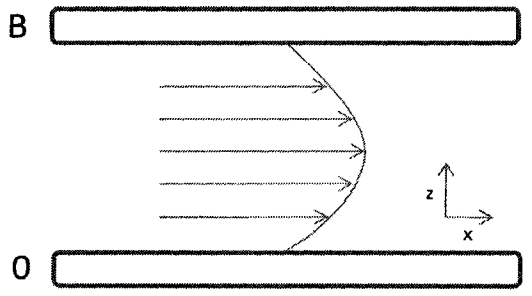

Figure 2.5: Flow profile in PPF cell. *Poiseuille flow between two parallel plates is characterized by a parabolic flow profile. For purposed of particle transport equations the lower plate is defined at z = 0, and the upper plate as z = B.*

Transport of non-motile, spherical particles is readily described by the convection-diffusion equation:

$$\nabla \cdot (\boldsymbol{u}C) = \nabla \cdot (\boldsymbol{D} \cdot \nabla C) - \nabla \cdot (\frac{\boldsymbol{DF}}{kT} C) \qquad \textit{Eq. 2.21}$$

where **u** is the particle velocity vector, C the particle concentration, **D** the particle diffusion coefficient tensor, **F** the force vector. The right hand terms from left to right describe diffusion and the influence of external forces (e.g., DLVO forces), respectively.

It is valuable to describe the convective –diffusion equation in terms of dimensionless variables (denoted by *) as listed in *Table 2.2.*

Table 2.2: Dimensionless numbers describing PPF hydrodynamics. *C_o is the bulk particle concentration, B is the height of the PPF, V_m is the flow velocity, D_∞ is the Stokes-Einstein diffusion coefficient, ρ is the fluid density, Q is the volumetric flow-rate, w is the flow cell chamber width, and υ is the kinematic viscosity.*

Variable	***Dimensionless Equivalent***	
Concentration	$C^* = \frac{C(H)}{C_o}$	*Eq. 2.22*
Height	$H^* = \frac{z}{a_p} - 1$	*Eq. 2.23*
Horizontal Coordinate	$x^* = \frac{x}{B}$	*Eq. 2.24*
Particle Size	$A^* = \frac{a_p}{B}$	*Eq. 2.25*
Peclet Number	$Pe = \frac{3V_m a_p^3}{2B^2 D_\infty}$	*Eq. 2.26*
Reynolds Number	$Re = \frac{\rho Q}{(w+B)\nu}$	*Eq. 2.27*

The Peclet number and Reynolds number are relevant in the selection of any representative flow geometry as they provide a means to match fluid dynamics. The Peclet number relates the rate of convection to the rate of diffusion, while the Reynolds number is the ratio of inertial forces to viscous forces.

Chapter Three

Materials & Methods

3.1 Bacteria & Cell Culture

Uropathogenic *E. coli* ATCC 700928 (more commonly known as CFT073) and *E. faecalis* ATCC 29212 were used in this study. *E. coli* CFT073 is a Gram negative clinical isolate from the blood and urine of a woman with acute pyelonephritis and its complete genome has been sequenced [44]. *E. faecalis* ATCC 29212 is a well-characterized Gram-positive uropathogenic bacterium isolated from urine. Pure cultures were maintained at -80 °C in Luria-Bertani Lennox broth (25 g/L) supplemented with 30% glycerol. Cultures were streaked onto LB agar plates that were then incubated for 24 h at 37 °C. For each experiment, a single colony from a fresh plate was used to inoculate 50 mL of LB broth (in a 150 mL Erlenmeyer flask). Cultures were incubated at 37 °C for 17 h at 200 rpm, then harvested by centrifugation at 5860*g* for 15 min (SS-34 rotor, Kendro) at 4 °C. The growth medium was decanted and the pellet was resuspended in phosphate buffered saline (PBS). Centrifugation and resuspension were repeated one additional time to remove any traces of growth media and metabolites. The concentration of the cell suspension was determined with a Helber (SV400, Proscitech, Australia) bacteria counting chamber and the suspensions were diluted accordingly to the desired final concentration of 1×10^8 CFU/mL in PBS (pH 7.4). Analytical reagent grade

chemicals (Fisher) and deionized (DI) (Milli-Q) water were used to prepare all solutions and media.

In selected experiments conducted to determine the effect of PAC on bacterial adhesion and bacterial surface properties, the final cell dilution was prepared using PBS supplemented with cranberry derived solubilized PACs (100 μg/mL). Briefly, dry PAC extract (obtained from A.B. Howell, Rutgers) was solubilized in DI to obtain a PAC stock solution (1.5 mg/mL). PAC supplemented PBS (PAC-PBS, 100 μg/mL) was then prepared by adding the appropriate volume of PAC stock to PBS.

3.2 Bacteria Viability

Plate counts were used to verify loss of cell viability when suspended in PAC-PBS. Cell suspensions were diluted in High Recovery Diluent (Oxoid), spread plated on R2A agar (Difco; in triplicate) and incubated for 24 hours (37°C) before counting. Cell viability was further verified using the BacLight Viability Kit (Invitrogen, Eugene, OR). Live and dead cells were then directly enumerated using fluorescent microscopy (IX-71, Olympus).

3.3 Bacteria Characterization

Microelectrophoresis (ZetaSizer Nano ZS, Malvern) was used to characterize the electrokinetic properties of the cells in PBS and PAC-PBS. Electrophoretic mobility (EPM) was measured at 22 °C using cell suspensions (4×10^7 cells/mL) prepared in either diluent. These measurements were repeated using at least three different samples of each bacterial suspension. Measured EPMs were converted to cell zeta potential using the Smoluchowski equation [45].

Individual components of bacterial surface free energies were determined from contact angle measurements on bacterial films with the polar liquids water and formamide and the apolar liquid diiodomethane. Contact angle measurements (sessile drop technique, OCA 20, Future Digital Scientific) were conducted on bacterial lawns formed on a

cellulose acetate membrane filter (0.45 μm, 47 mm diameter, GE Osmonics) using the method described by Van Oss and others [38, 46]. At least four measurements were made on each filter, and at least three filters were used for each condition at ambient temperature 22 °C.

The nominal size of the bacteria was determined by analyzing images taken in an inverted fluorescent microscope (IX-71, Olympus) operating in phase contrast mode. An image processing program (ImageJ, NIH) was used to determine the average lengths of the major and minor axes of the cells and the resulting equivalent spherical diameter.

3.4 Adsorption of PAC on Polymer Surfaces

A quartz crystal microbalance with dissipation monitoring (QCM-D) was used to verify adsorption of cranberry derived PACs onto a biomaterial surface (note: only PVC coated quartz crystals were available from the manufacturer). The QCM-D E4 unit (Q-Sense AB, Västra Frölunda, Sweden) consists of a measurement chamber platform that can hold 4 sensor flow modules. Each flow module holds a 5 MHz AT-cut quartz sensor crystal with a PVC coated surfaces and is configured such that the flow is parallel to the crystal surface (as in the parallel plate flow cell). Prior to mounting in the flow modules, the PVC coated crystals were soaked in DI and dried with ultra-high purity N_2 gas. The clean dry crystals were mounted in a flow chamber, and PBS was drawn through the chamber with a peristaltic pump (150 μL/min, Ismatec) until baseline was achieved (i.e., the measured change in frequency was less than 1 Hz/hour). PAC-PBS (100 μg/mL) was then drawn through the chamber for 30 min (150 μL/min), followed by an equivalent injection of PBS (150 μL/min). Finally, a mild detergent (1% Hellmanex in DI, 300 mL/min, 10 min) was drawn through the chamber followed by a rinse with DI (300 mL/min, 10 min). During the QCM-D experiment, the temperature inside the measurement chamber was maintained at 22 °C. The thickness and density of the adsorbed PAC film were assumed to be uniform. Analysis of the QCM-D data was done using the Q-Tools program (Q-Sense AB).

3.5 Polymer Surface Characterization

Zeta potential of the PVC and PTFE biomaterials was determined by streaming potential analysis conducted on thin rectangular coupons prepared from the same materials used for flow cell experiments (Biosurface Technologies). The rectangular coupons were mounted inside a parallel plate flow cell (Model FC81, Biosurface Technologies) of comparable dimensions to the one described in *Section 3.6*, but specially designed for thin rectangular coupons (L×W×H = 40.6 × 11.4 × .203 mm). After mounting a coupon inside the flow cell, the coupon was equilibrated with PBS (control) or PAC-PBS (to allow adsorption of PAC onto the biomaterial) for 10 min (0.5 mL/min). The treated coupon was then removed from the flow cell and mounted in the clamping cell of a streaming potential analyzer (EKA, Brookhaven Instruments Corp., NY). The streaming potential measurements were conducted by pumping PBS across the biomaterial surface. The biomaterial zeta potentials were determined from the measured streaming potentials using the analysis presented by Walker et al [47].

Individual components of biomaterial surface free energies were determined from contact angle measurements on the biomaterial coupons as described above for bacterial films. Contact angle measurements (sessile drop technique, OCA 20, Future Digital Scientific) were conducted on PVC or PTFE coupons after they had been equilibrated with PBS or PAC-PBS for 10 min as described above. At least four measurements were made on each coupon (at ambient temperature 22 °C), and at least two coupons were used for each condition.

3.6 Bacteria and Particle Adhesion Experiments

Bacterial adhesion to two common biomaterials was examined using a dual channel parallel plate flow cell (dimensions, L×W×H = 39.5 × 13 × 0.32 mm, Model FC271, Biosurface Technologies). Clean PVC or PTFE disks (diam. 14 mm, Biosurface Technologies) were mounted in the flow cell and the system was equilibrated with PBS using a syringe pump (Model 200, KD Scientific) at 0.5 mL/min for a duration of 10 min. This flow rate provided a Reynolds number of 0.6, a shear rate of 37 . Bacterial

suspensions (1×10^8 CFU/mL) were then injected into the flow cell (0.5 mL/min, 10 min), followed by an equivalent injection of PBS alone (0.5 mL/min, 10 min) to remove any unbound cells from the system. The PVC or PTFE disks were then carefully removed from the flow cell, stained with DAPI (4',6-diamidino-2-phenylindole) (100 μL at 100 μg/mL) and incubated in the dark for 10 min. The PVC or PTFE disks were then imaged by fluorescence microscopy (IX-71, Olympus), and the attached bacteria were enumerated with image analysis software (ImagePro). At least 30 images were taken of each coupon at 20× magnification. Four separate treatments were used in the adhesion experiments: (i) control: bacteria suspended in PBS were injected into the flow cell; (ii) bacteria only treated with PAC: bacteria were resuspended in PAC-PBS (100 μg/mL) for a duration of 10 min to allow PAC adsorption onto the cell surfaces, the suspension was centrifuged, the supernatant decanted, and cells were resuspended in PBS prior to injection in the flow cell; (iii) biomaterials only treated with PAC: prior to injecting the bacteria into the flow cell, a PAC-PBS solution (100 μg/mL) was injected (0.5 mL/min, 10 min) to allow adsorption of the PAC onto the biomaterial surface, followed by injection of PBS alone (0.5 mL/min, 10 min); (iv) biomaterials and bacteria treated with PAC: bacteria resuspended in PAC-PBS (100 μg/mL) were directly injected into the flow cell. These experiments were conducted with the two bacteria selected (*E. coli* CFT073 and *E. faecalis).* To better understand the mechanism by which PAC influences the adhesion of the bacteria, an additional set of flow cell experiments was conducted using fluorescent blue sulfate latex microspheres (Invitrogen, Eugene, OR). The microspheres were selected to be similar in size to the bacteria (1.0 μm diam.) and experiments were conducted for the four treatments described above using a microsphere concentration of 1×10^7 particles/mL. All bacteria and microsphere adhesion experiments were conducted at ambient temperature (22 °C).

Kinetics experiments were performed using latex particles with the flow cell apparatus as described above with real-time fluorescence imaging. Images were taken at 20× magnification every 10 seconds for the duration of the particle injection. Enumeration was done with image analysis software (ImagePro). Kinetics experiments were repeated three times under control conditions and PAC supplemented conditions (100 μg/mL).

3.7 Protein Expression

Bacterial metabolic changes in response to PAC supplemented growth media was evaluated with SDS-PAGE. *E. coli* CFTO73 was cultured for six consecutive generations in 50 mL of LB broth (in 150 mL Erlenmyer flasks) at 37° C rocking at 200 RPM with and without the presence of PAC (100 μg/mL). Bacteria were harvested after 6 hours of growth by centrifugation at 6000 × g at 4° C for 15 min, then resuspended in PBS (pH 7.4). Subsequent cultures were inoculated with 1 mL of the previous culture and treated similarily. Bacteria lysis was achieved with Cellytic tablets (Sigma) with incubation at 37° C for 20 minutes and intermittent vortexing. Protein concentration of whole cell lysate was assayed with Quick Start Bradford Protein Assay (Bio-Rad). Lysate was electrophoresed at 200V in a 10% SDS-PAGE gel for 40 minutes. The gel was then silver stained (PageSilver, Fermentas). Gel was then placed on filter paper and scanned (HP Deskjet F300 Series).

Chapter Four

Results & Discussion

4.1 Effect of PAC on Bacteria Growth and Viability

The interest of PAC in the prevention of infection lies in its mechanistic action as an anti-adhesive compound without antibacterial effects. Antibacterial properties have been reported at concentrations greater than 200 μg/mL while anti-adhesive effects have been observed at concentrations as low as 25 μg/mL. The anti-adhesive properties of PAC have only been demonstrated against bacteria adhesion to mammanlian cells. This is the first investigation of PAC inhibited adhesion of bacteria to biomaterial surfaces. For this study a working concentration of 100 μg/mL was selected and tested for any effects on bacterial growth and viability.

PAC did not inhibit the growth of *E. coli* CFTO73 when growth media was supplemented at the working concentration. *Figure 4.1a* depicts that in fact the opposite effect was observed where growth in PAC media was faster, and final concentrations of cells at stationary phase were higher (8×10^9 CFU/mL in PAC supplemented LB and 4×10^9 CFU/mL in LB). Similar results were observed for *E. faecalis* growth where viability was determined at $2.0 \pm 0.2 \times 10^9$ CFU/mL in PAC-PBS as compared to $1.8 \pm 0.1 \times 10^9$ CFU/mL in PBS. When bacteria were grown without PAC then resuspended and

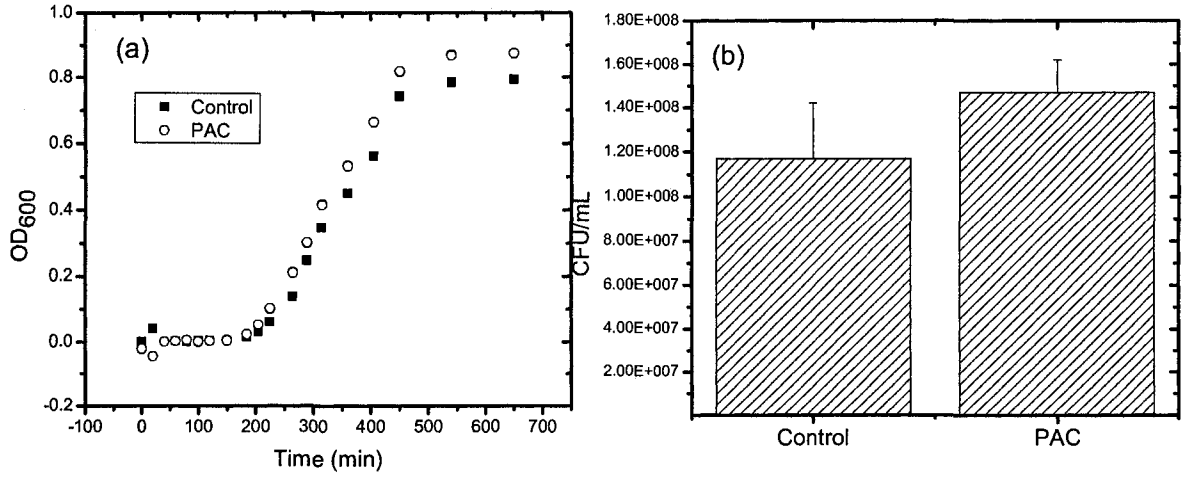

Figure 4.1: Growth and viability of E. coli CFT073 in the presence of PAC. *(A) Growth curve of diluted culture demonstrating a slightly increased growth rate of E. coli in PAC supplemented LB. (B) Viability of E. coli incubated with PBS supplemented PAC for 30 minutes, no significant differences are evident.*

incubated in PAC supplemented PBS there were no significant differences in viability when determined with plate counting and live/dead staining for either *E. coli* ($1.4 \pm 0.2 \times 10^7$ CFU/mL and $1.4 \pm 0.1 \times 10^7$, in PBS and PAC-PBS respectively, *Figure 4.1a*) or *E. faecalis* Similarly, in the case of *E. faecalis* ($1.2 \pm 0.2 \times 10^7$ CFU/mL and $1.3 \pm 0.2 \times 10^7$ CFU/mL, in PBS and PAC-PBS respectively).

4.2 Influence of PAC on Surface Properties

Surface free energies of bacterial lawns and polymer surfaces, before and after exposure to PAC, obtained from sessile drop contact angle measurements are presented in Table 4.1. The bacterial strains were determined to be hydrophilic ($\theta_w < 60°$), with PAC treatment causing an increase in *E. coli* hydrophobicity and having no significant effect on *E. faecalis*. Ionic and polar groups on surfaces lead to an increased affinity for water and may inhibit adhesion due to hydration effects. It has been reported that hydrophobic effects dominate electrostatic effects in bacterial adhesion. Increase of hydrophobicity is often associated with increased bacterial adhesion to hydrophobic and hydrophilic surfaces. The reverse trend was observed with PAC treated polymers, where both PVC and PTFE tended to be more hydrophilic, and therefore more repulsive to adhesion. With

***Table 4.1*: Summary of bacterial and polymer surface properties** *with and without the presence of PAC. Surface free energy values as determined from contact angles on bacterial lawns obtained using the sessile drop technique. Contact angles are presented as θw, θf, and θm, water, formamide, and diiodomethane respectively. Surface free energies are presented as γ^T, γ^{LW}, γ^{AB}, γ^+, and γ^-, for total surface free energy, Lifshitz-van der Waals, acid base, electron acceptor, and electron donor components, respectively. Electrophoretic mobility (for bacteria) and streaming potential (for polymer surfaces) were used to calculate ζ-potential using the Smoluchowski-Helmholtz approach.*

	Contact Angle (°)[a]			Surface Tension Components (mJ/m^2)					EPM	ζ	a_p
	θ_w	θ_f	θ_m	γ^T	γ^{LW}	γ^{AB}	γ^+	γ^-	(μm cm/Vs)	(mV)	(μm)
Organism/Particle											
E. coli	24 (2.6)	22 (2.6)	51 (4.6)	53.7	33.9	9.9	2.0	48.5	-1.96 (0.2)	-21.8 (1.7)	1.75 (0.5)
E. coli + PAC	49 (3.0)	30 (5.6)	49 (4.3)	50.4	35.0	7.7	2.5	24.1	-2.08 (0.1)	-23.1 (0.6)	1.77 (0.5)
E. faecalis	26 (5.7)	33 (7.7)	49 (2.2)	47.1	34.7	6.2	0.7	54.7	-1.38 (0.1)	-15.3 (0.7)	0.79 (0.2)
E. faecalis + PAC	24 (3.1)	25 (4.3)	50 (1.5)	52.4	34.5	9.0	1.6	50.4	-1.41 (0.1)	-15.7 (1.0)	0.70 (0.1)
Latex	-	-	-	-	-	-	-	-	-2.83 (0.2)	-39.2 (2.1)	-
Latex + PAC	-	-	-	-	-	-	-	-	-1.48 (0.1)	-20.5 (0.6)	-
Biomaterial											
PVC	87 (3.9)	79 (3.4)	45 (3.3)	36.7	36.7	0.0	10.5	0.0	-	-24.9 (4.0)	-
PVC + PAC	66 (3.4)	55 (5.9)	45 (1.9)	38.7	37.0	4.1	19.1	0.9	-	-28.3 (3.9)	-
PTFE	108 (2.5)	92 (4.3)	53 (6.5)	32.3	32.3	0.0	1.4	0.0	-	-29.2 (3.9)	-
PTFE + PAC	95 (1.3)	73 (4.7)	92 (4.3)	28.9	27.7	0.2	1.5	0.6	-	-30.3 (4.5)	-

[a] Contact angles were measured using water (θ_w), formamide (θ_f), and diiodomethane (θ_m).
[b] The values in parentheses are standard deviations

low values for the electron donating components for bacteria and low values for the electron accepting components of surface energy, the total free surface energy of each measurement is dominated by Lifshitz-van der Waals interactions.

Zeta-potentials of bacteria in PBS electrolyte as calculated from electrophoretic mobility using the Smoluchowski-Helmholtz approach are presented in Table 4.1. The high ionic strength of PBS (147 mM) is a limitation in the measurement of electrophoretic mobility as very low voltages must be applied across the solution in order to avoid damaging the bacteria. Low voltage leads to slow movement of bacteria through the electrolyte during measurement resulting in a wider distribution of electrophoretic mobilities. For this reason the Malvern ZetaSizer functions in monomodal mode and eliminates the slow reversal phase involved with measuring electrophoretic mobility in lower ionic strength

electrolyte. There was no significant change in bacterial ζ-potential with PAC treatment, implying that PAC molecules are not causing measurable changes in bacterial surface potential.

4.3 PAC Adsorption onto PVC

In elucidating mechanisms of action it was necessary to understand how polymer surfaces were coated with PAC. In order to test the hypothesis of direct PAC stabilization on these surfaces, a quartz crystal microbalance (QCM) installed with PVC coated quartz crystals was used to measure film formation. With an assumed film density of 1050 kg/m^3, an approximately 5 nm film formed on the crystal surfaces with a calculated mass of nearly 600 ng/cm^2 (*Figure 4.2*). PVC was readily and reversibly coated by PAC with no steady state achieved over the course of the experiment suggesting some multilayering of the molecules. These properties are suggestive of van der Waals intermolecular forces mediating physical adsorption rather than PAC adhering to the surface via covalent bonding or chemisorption.

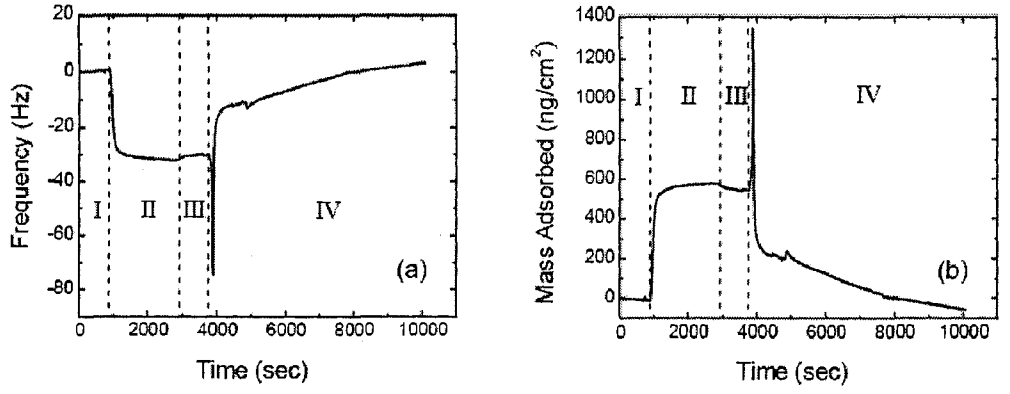

Figure 4.2: QCM data of PAC adsorption on PVC. *Mass deposition (B) as calculated using Sauerbrey's equation for rigid films, from QCM frequency response (A) during PAC adsorption to PVC coated crystals. (I) Baseline was achieved in PBS. (II) PAC supplemented PBS was flowed through the sytem (100 μg/mL), (III) PBS is injected; (IV) 0.1% Hellmanex is injected.*

4.4 Examining Adhesion in the Presence of PACs

Parallel plate flow cell experiments were performed to determine the effectivity of PAC in preventing the adhesion of bacteria to biomaterial surfaces. Figure 4.3 summarizes the results of the bacterial adhesion experiments conducted with both biomaterials, where the four treatments are indicated as follows: (i) control (CTRL), (ii) bacteria only treated with PAC (BAC); (iii) biomaterial only treated with PAC (MAT), and (iv) biomaterials and bacteria treated with PAC (BOTH). Overall, the data shows that PAC inhibited bacterial attachment under all conditions, whether only the biomaterial or bacteria or both surfaces had been treated. In *Figure 4.3a,* the results show 1.6 and 1.5-fold reductions in the extent of *E. coli* attached to PVC when either the substrate or the bacteria is treated with PAC, respectively. Similarly, 1.7 and 1.8-fold reductions in attached *E. coli* cells were observed for experiments conducted with PTFE when either the material or the cells were treated with PAC. When both the bacteria and the biomaterial were PAC treated, the extent of *E. coli* attachment to PVC and PTFE was 1.8 and 2.1-fold lower, respectively. To our knowledge, this is the first evidence that PAC has the ability to prevent the adhesion of uropathogenic *E. coli* to biomaterials. The effects of PAC were even more pronounced when *E. faecalis*, a Gram-positive microorganism, was tested (*Figure 4.3b*). Results of experiments examining the influence of PAC on *E. faecalis* adhesion reveal 2.0-fold and 1.4-fold reductions in the extent of bacterial adhesion onto PVC when either the biomaterial (MAT) or the microorganism (BAC) is treated with cranberry PAC, respectively. Experiments conducted with *E. faecalis* and PTFE show an even greater effect, whereby the extent of bacterial attachment decreases by 56% when the biomaterial is treated with PAC prior to injection of the bacteria into the PPFC. When both the bacteria and the biomaterial were PAC treated, the reduction in *E. faecalis* adhesion to PVC and PTFE was 90% and 88% lower, respectively. This is also the first evidence of PAC preventing the adhesion of a Gram-positive microorganism. For both bacteria-biomaterial systems, maximum inhibition of adhesion occurred when both the biomaterial and the bacteria were treated with PAC, suggesting that the compound was acting at both surfaces.

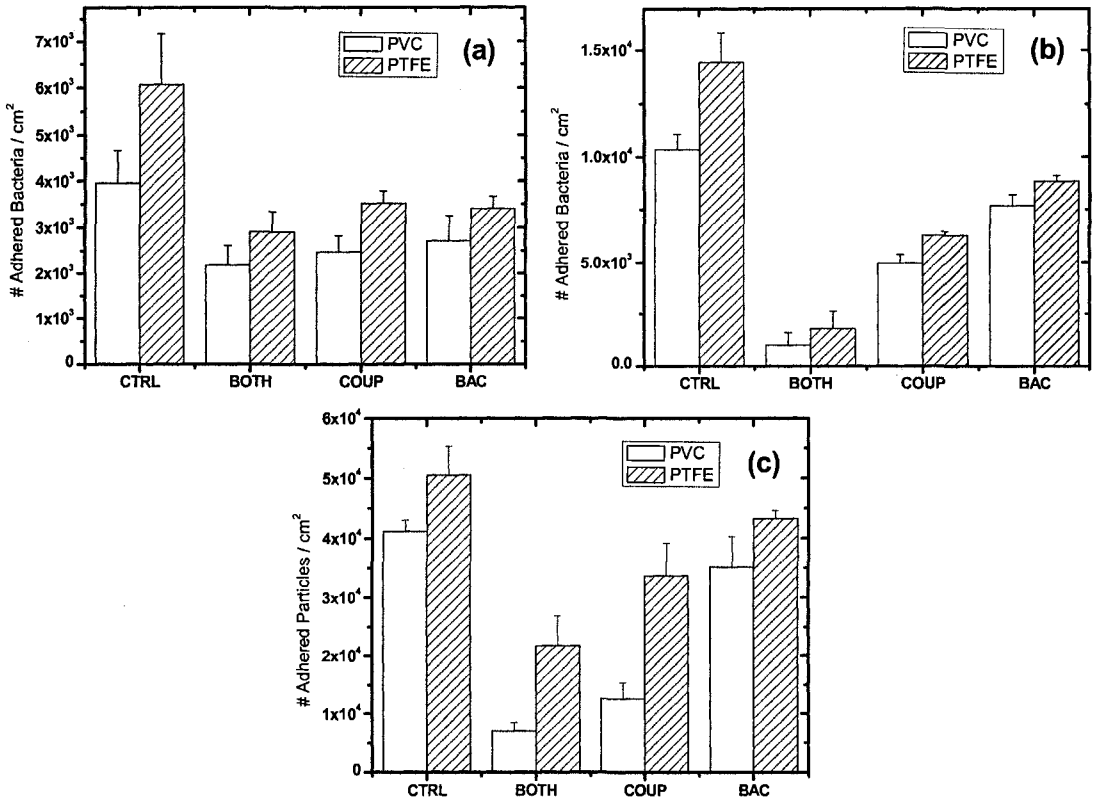

Figure 4.3: ***Results from parallel plate flow cell experiments****: (A) E. coli CFTO73, (B) E. faecalis ATCC 29212, (C) Latex microspheres. Conditions are abbreviated as Control (CTRL), PAC treatments of coupon and bacteria (BOTH), coupon treated (COUP), and bacteria treated (BAC).*

To investigate the potential of non-specific action, flow cell experiments were repeated with latex microspheres, thereby eliminating any biospecific effects. Reductions in adhesion were observed ranging from 1.2 to 5.8-fold (*Figure 4.3c and Figure 4.4*). This demonstrates that non-biospecific mechanisms, at least in part, account for PAC effects. Zeta-potential measurements of latex microspheres became more positive in the presence of PAC (*Table 4.1*) that would normally lead to increased deposition due to a decrease in the EDL thickness based on classical DLVO theory. However the opposite behaviour was observed, providing evidence that PAC effects are not electrostatically mediated, probably due to the high ionic strength of PBS.

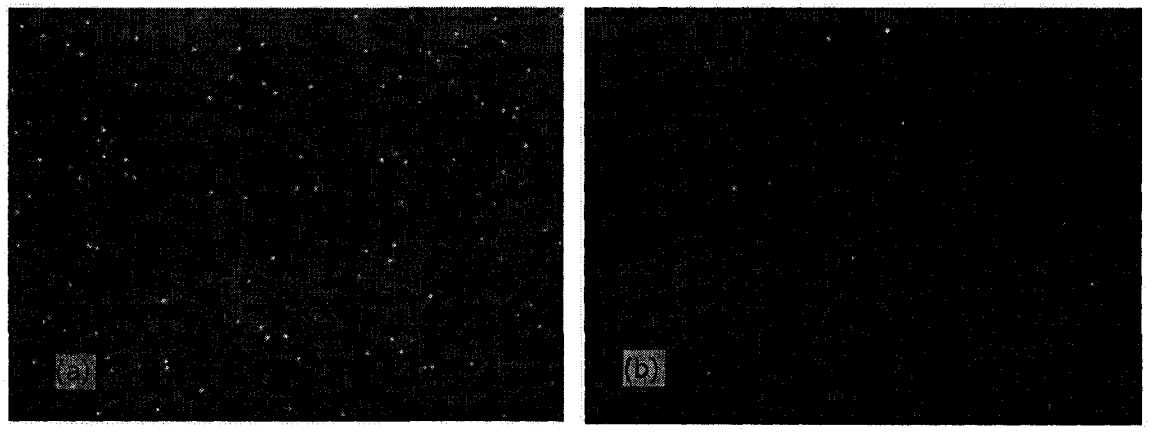

***Figure 4.4**: Representative microscope images (20× magnification) of PTFE surface following flow cell experiments with latex microspheres. (a) in the absence of PAC ("CTRL" condition), and (b) in the presence of PAC ("BOTH" condition).*

This new evidence of PAC functioning independent of the Gram staining of the bacteria is suggestive of nonspecific mechanisms of action, unlike those previously suggested in the literature with respect to adhesion of *E. coli* to mammalian cells [16, 17].

4.5 Kinetics and Dose Response of Microsphere Adhesion

With the knowledge that surface effects were important in the function of PAC in preventing adhesion further experiments were performed with latex microspheres in order to better understand this mechanism. A dose response where varying PAC concentrations were used in treating both PTFE and latex particles demonstrated that with increasing PAC concentration fewer particles deposited on the surface. The effect was not as obvious with PVC (*Figure 4.4a*). The zeta-potential of latex increased with the addition of PAC to electrolyte, and bound strongly (noted as measurements were taken after centrifugation and resuspension in fresh electrolyte), however zeta-potential did not change significantly between low and high PAC concentrations (*Figure 4.4b*).

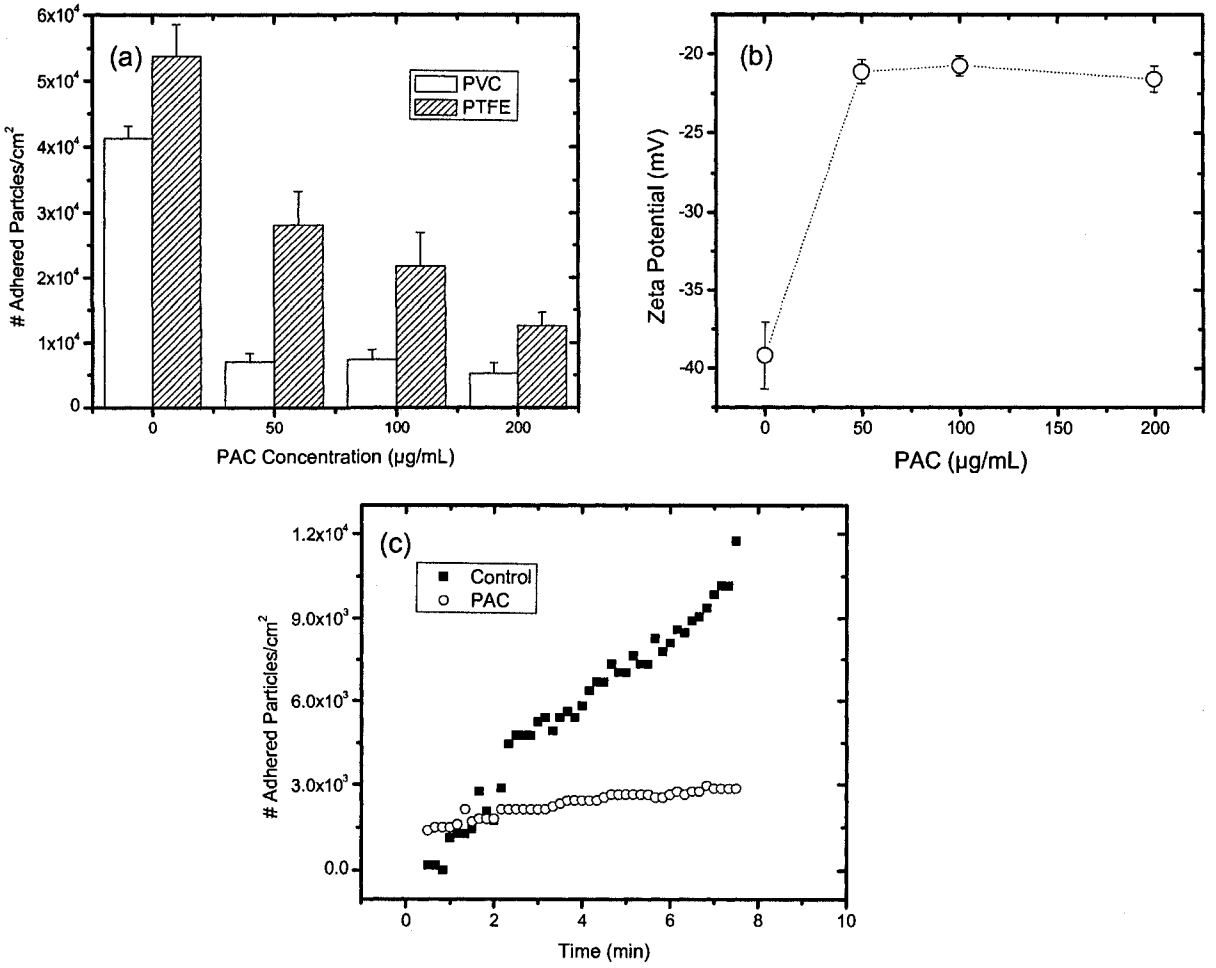

Figure 4.5: Results from latex microsphere experiments. *(A) PAC dose response against latex microsphere adhesion to PVC and PTFE coupons. (B) Zeta potential of latex microspheres incubated with PAC then resuspended in PBS. (C) Adhesion kinetics of latex microspheres on PVC with and without PAC supplementation.*

Kinetics experiments were then performed capturing adhesion of latex microspheres to PVC coupons as a function of time. The first finding of this experiment was that PAC decreased the rate of initial adhesion, from 1.4×10^3 particles per minute to 2.0×10^2 particles per minute as determined by the slopes of the curves in *Figure 4.4C*. The second finding was that binding of particles in the presence of PAC appeared to be weaker as particles adhered for some time then detached - a phenomenon that was not observed in the absence of PACs.

4.6 Application of Colloidal Theory to Bacterial Adhesion

The observed significant influence of PAC on a non-biological particle demonstrates that, at least in part, non-biospecific mechanisms account for its antiadhesive properties on biomaterials. Furthermore, in contrast to the results obtained with the two bacteria, PAC treatment resulted in lower absolute values of zeta potential for the latex particles (*Table 4.1*). Within the context of the classical DLVO theory of colloidal stability, a particle with a lower absolute potential will experience a lower extent of electrostatic repulsion upon approach to an oppositely charged surface, thereby leading to a greater extent of attachment [39, 48, 49]. However, the opposite behavior is observed in *Figure 4.4a*, whereby the degree of particle deposition onto the biomaterial surfaces is lower in the presence of PAC. This observation suggests that PAC effects are not electrostatically mediated at the conditions examined here.

To better understand the mechanisms controlling the observed bacterial deposition behavior, the xDLVO model was used to calculate bacteria-biomaterial interaction energies. *Figure 4.6* shows representative xDLVO interaction energy profiles for the *E.coli*-PVC system, where the total interaction energy (V_T) was evaluated as the sum of equations 1, 7, and 9. The calculations reveal sizable energy barriers (on the order of 11,000kT) for the "CTRL" and "MAT" conditions, but no energy barriers to deposition in the primary energy minimum are expected for the "BAC" and "BOTH" conditions. Hence, based on the xDLVO interaction energy calculations, the *E. coli* is not expected to deposit on the PVC surface when there is no PAC treatment, nor when the biomaterial alone is treated with PAC. In contrast, the cells are expected to deposit extensively on the PVC surface for the "BAC" and "BOTH" conditions. Despite these xDLVO predictions, however, *E. coli* adhesion is highest in the absence of PAC and lowest when both the biomaterial and the bacteria are treated with PAC. PAC treatment, nor when the biomaterial alone is treated with PAC. In contrast, the cells are expected to deposit extensively on the PVC surface for the "BAC" and "BOTH" conditions. Despite these xDLVO predictions, however, *E. coli* adhesion is highest in the absence of PAC and lowest when both the biomaterial and the bacteria are treated with PAC.

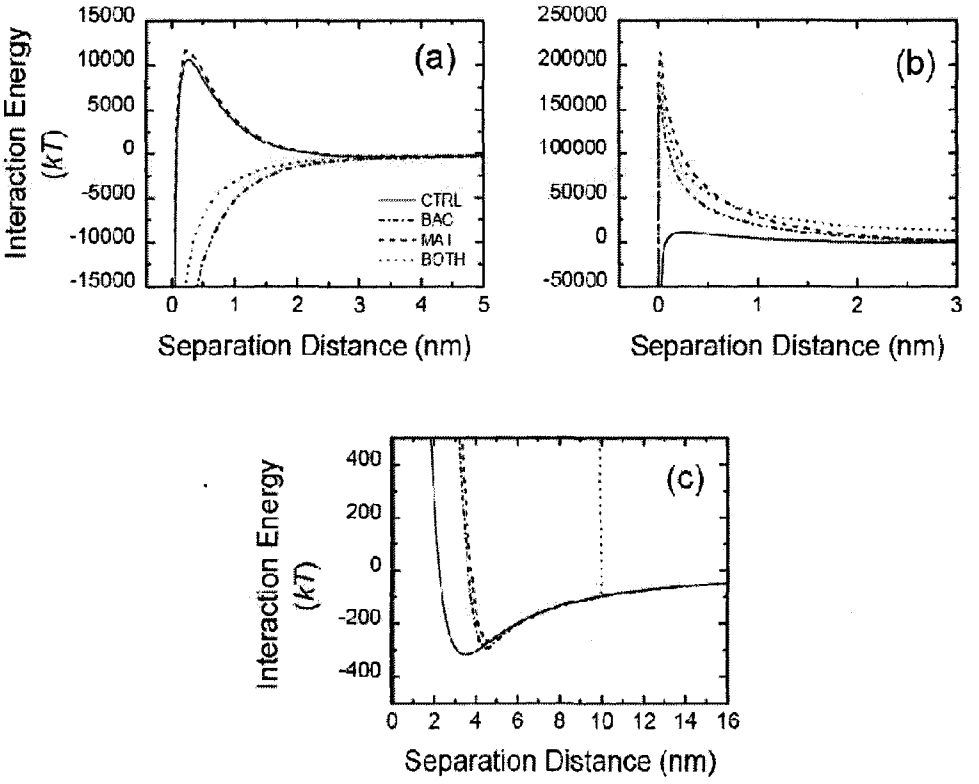

Figure 4.6: *epresentative calculated interaction energy plotted as a function of separation distance for E. coli approaching a flat PVC surface using (a) the xDLVO model; (b) the Steric model; and (c) the Steric model replotted on a different scale to highlight the presence of the secondary energy well. Measured zeta potentials (Table 4.1), calculated surface tension components (Table 4.1) and calculated Hamaker constants (Table 4.2) were used to determine interaction energies.*

Table 4.2 summarizes the key parameters calculated using the xDLVO model for the four different bacteria-biomaterial systems; namely, the maximum height of the energy barrier (Vb), and the Hamaker constant (A). The xDLVO model predicts no energy barriers to deposition when both surfaces are treated with PAC. Yet, the least amount of bacterial adhesion was observed for these conditions (*Figure 4.3*). In contrast, relatively high values of Vb are predicted for the control treatment for all four systems, yet the extent of attachment is always greatest for this condition. Clearly, the *E. coli* and *E. faecalis* deposition behavior observed in the PPFC experiments is not well described by the xDLVO model.

Table 4.2: xDLVO and steric model energy barriers. *Energy barriers associated with xDLVO theory (Eq. 2.1 + Eq. 2.2 + Eq. 2.14) and the steric model (Eq. 2.1 + 2.14 + 2.19/20). A value of 0 indicates that no energy barrier was predicted.*

	Predicted Energy Barriers (V_b) and Calculated Hamaker Constants (A)							
	Treatment							
Bacteria-Biomaterial System	CTRL[a]		BAC		MAT		BOTH	
	V_b (kT)	A (J)	V_b (kT)	A (J)	V_b (kT)	A (J)	V_b (kT)	A (J)
E. coli-PVC								
xDLVO model[c]	10,600	3.0×10^{-20}	0[b]	3.0×10^{-20}	11,600	3.0×10^{-20}	0	3.0×10^{-20}
Steric model[d]	-	3.0×10^{-20}	165,000	3.0×10^{-20}	213,400	3.0×10^{-20}	187,200	3.0×10^{-20}
E. coli-PTFE								
xDLVO model	1,300	2.9×10^{-20}	0	2.9×10^{-20}	0	2.7×10^{-20}	0	2.8×10^{-20}
Steric model	-	2.9×10^{-20}	149,000	2.9×10^{-20}	199,400	2.7×10^{-20}	166,600	2.8×10^{-20}
E. faecalis-PVC								
xDLVO model	5,500	3.0×10^{-20}	4,800	3.0×10^{-20}	6,300	3.0×10^{-20}	0	2.9×10^{-20}
Steric model	-	3.0×10^{-20}	88,900	3.0×10^{-20}	91,000	3.0×10^{-20}	94,000	2.9×10^{-20}
E. faecalis-PTFE								
xDLVO model	200	2.9×10^{-20}	500	2.9×10^{-20}	0	2.8×10^{-20}	0	2.8×10^{-20}
Steric model	-	2.9×10^{-20}	83,300	2.9×10^{-20}	81,600	2.8×10^{-20}	87,600	2.8×10^{-20}

[a] For the control condition (i.e., no PAC), only the XDLVO model was used for the interaction energy calculations.

[b] "0" indicates that no energy barrier is predicted for this condition.

[c] The XDLVO model considers the sum of equations 1, 7, and 9.

[d] The Steric model considers the sum of equations 1, 7, and 13.

Careful inspection of the data presented in *Figure 4.3c* reveals general agreement between predictions based on the xDLVO model and experimental results in the absence of PAC (i.e., for the control condition). Specifically, a greater absolute number of cells deposit onto the PTFE surface in comparison to the PVC surface. For instance, for the control condition on PVC, there are 1×10^4 cells of *E. faecalis* attached per square cm, whereas there are 1.4×10^4 cells/cm^2 of *E. faecalis* attached on PTFE under the same conditions. Likewise, the calculated value of Vb is significantly greater (~5,500kT) for the interaction of *E. faecalis* with PVC in comparison to that predicted for the interaction of *E. faecalis* with PTFE (200kT). However, as described previously, the xDLVO model fails to predict the observed bacterial adhesion behavior when PAC is used to treat the bacteria and/or biomaterial surfaces. Steric stabilization is a well-known phenomenon in the colloid literature [50-52]. Adsorbed layers of polymer (such as cranberry derived PAC) on the surfaces of biocolloids (e.g., bacteria) or collector surfaces (e.g.,

biomaterials) can give rise to steric interactions upon approach of the cell to the biomaterial surface. To evaluate the potential role of steric interactions in the four bacteria-biomaterial systems, the Steric model (described in *section 2.6.5*) was used to calculate the overall interaction energy profiles for all experimental conditions considered. Two parameters (s and L) in the Alexander-de Gennes equation (*Eq. 2.19/20*) were estimated from the QCM data (*Figure 4.2*). The length of the polymer chains was assumed to be equivalent to the film thickness (L = 5 nm) determined using QCM by assuming that PAC formed relatively linear and neutral chains in PBS. Polymer spacing on the PVC surface was evaluated using the total estimated deposited PAC mass from the QCM experiment and a PAC molecular weight of 15 kDa. From this data, the density of polymers was determined as 2.1×10^3 molecules/cm^2, with a spacing s of 2.2 nm between them. To illustrate the effect of steric interactions on all four systems, these estimated parameters (s and L) were also used in the steric model calculations related to the PTFE- and bacteria-coated surfaces. Representative interaction energy profiles calculated using the Steric model (sum of *Eq. 2.1 + 2.14 + 2.19/20*) for the *E. coli*-PVC system are presented in *Figure 4.6*b. The graph shows significantly different predictions from those evaluated using the xDLVO model. Most clearly, calculated heights of the energy barrier (Vb) are at least an order of magnitude greater when PAC is used to treat at least one of the surfaces (bacteria or biomaterial). Values of Vb calculated using the steric model for the four different bacteria-biomaterial systems are summarized in *Table 4.2*. When steric interactions (V^{ST}) are considered, the calculated heights of the energy barrier (Vb) are significantly greater for PAC conditions than for the control conditions (for all four bacteria-biomaterial systems). Comparison of the Vb values calculated using the steric model (*Table 4.2*) with the *E. faecalis* adhesion data presented in *Figure 4.3b* reveals good qualitative agreement between theoretical predictions of adhesion and the experimental results. Specifically, the steric model predicts larger barriers to adhesion (on the order of 87,600 to 94,000kT) for the dual treatment condition ("BOTH") in contrast to the conditions where only one (bacteria or biomaterial) or no surface was treated with PAC (values range from 81,600 to 91,000kT).

Accordingly, the treatment with the lowest number of attached *E. faecalis* cells is that where both the bacteria and the biomaterial surfaces are treated with PAC *(Figure 4.3b)*. Likewise, the greatest extent of *E. faecalis* adhesion is observed for the control condition where the lowest energy barrier to deposition is expected (for both biomaterials examined). The two remaining treatments ("BAC" and "MAT") exhibit cell attachment in between that observed for the "CTRL" and "BOTH" conditions, and correspondingly, lower values of V_b. Another trend that is observed in the Steric model calculations presented in *Table 2* is the generally greater values of V_b for the *E. coli* in comparison to *E. faecalis* (for the three treatments involving PAC). As noted previously for the control condition, these greater energy barriers to deposition are in agreement with the observed adhesion data, whereby we observe more overall adhesion (in terms of number of cells attached) of the *E. faecalis* in comparison to the *E. coli*. Furthermore, it is interesting to note that the Steric model calculations predict larger values of V_b for deposition onto PVC in comparison to PTFE. Likewise, the results of the PPFC experiments reveal greater attachment to PTFE versus PVC. Comparison of the experimental adhesion data with theoretical predictions of bacteria-biomaterial interaction energies based on the steric model suggests that steric stabilization may be an important mechanism by which PAC inhibits bacterial adhesion to inert surfaces. Although the theoretical predictions of the bacteria-biomaterial interaction energy profiles are generally in good agreement with experimental results for the two *E. faecalis* biomaterial systems, this is not always the case observed for *E. coli*. In the case of *E. coli* interactions with PVC or PTFE, the calculated heights of the energy barrier are not always in qualitative agreement with the experimental data in *Figure 4.3a*. For instance, for the *E. coli*-PTFE system, the steric model predicts a greater value of V_b for the "MAT" treatment (199,400kT) than for the "BOTH" treatment (166,600kT), yet a greater number of cells adhered on the PTFE surface for the "MAT" condition (*Figure 4.3a*). This observation suggests that there may be another mechanism playing a role in the observed bacterial adhesion behavior. The better qualitative agreement between theoretical predictions and the experimental results for *E. faecalis* in comparison to *E. coli* may also be linked to the nature of the organisms. *E. faecalis* is a Gram-positive organism that has a more spherical shape which is better suited to the theoretical calculations.

Values of V_b determined using the steric model are generally on the order of 81,000kT or greater (when an energy barrier is present) (*Table 4.2*). The xDLVO model also predicts sizable energy barriers for the control treatment. Based on these calculations, bacteria are not expected to deposit on the biomaterial surfaces (i.e., overcome the repulsive energy barrier) except in the conditions where V_b is on the order of 0 to 25kT. Despite these theoretical predictions, however, bacterial adhesion is observed even when both surfaces are treated with PAC.

There is increasing evidence in the literature pointing to the importance of the secondary energy minimum in controlling particle and microbial deposition onto inert surfaces [53-56]. The secondary energy well in the bacteria-surface interaction energy profile is located at a greater separation distance than that of the repulsive energy barrier. In *Figure 4.6c*, where the steric model interaction energy profiles are replotted on a different scale, we note the presence of a secondary energy well for each treatment. *Table 4.3* summarizes the predicted depths of the secondary energy well based on calculations using the XDVLO and steric models, for control and PAC treatments, respectively. Because the heights of the repulsive energy barrier are so great, it is much more likely that the bacteria are being retained in the secondary energy minimum rather than overcoming an energy barrier to deposit in the primary energy minimum. Indeed, the observed bacterial adhesion behaviour (*Figure 4.3*) is in strong qualitative agreement with the predicted depths of the secondary energy minimum for each system examined, whereby deeper wells are associated with a greater extent of adhesion. For instance, in the case of *E. coli* interacting with PTFE, the shallowest secondary energy well (89kT) is linked with the lowest extent of adhesion ("BOTH" treatment), whereas the deepest well (387kT) is associated with the greatest number of attached cells ("CTRL" treatment). The same trend is followed for the three other bacteria-biomaterial systems. The data in *Table 4.3* also indicate that the deeper energy wells are located at smaller separation distances (h), thereby facilitating bacterial attachment to the biomaterial surface.

Deposition in the secondary energy minimum is reversible, meaning that retained particles or bacteria may be released during the PPFC experiments. An additional series of PPFC experiments were carried out using the latex microspheres whereby the deposition and release of particles onto PVC was monitored in real-time. Direct observation of microsphere deposition onto PVC for the "CTRL" and "BOTH" treatments revealed detachment of the microspheres over the course of the experiment only for the condition where PAC was used (data not shown). This microscopic observation of particle detachment provides evidence for a reversible attachment mechanism, such as retention in the secondary energy minimum.

Although the predicted depths of the secondary energy well are in good qualitative agreement with the experimental data, a few inconsistencies can still be observed in the overall trends. These inconsistencies may be attributed to the influence of surface charge heterogeneities on the bacteria or biomaterial surface, or nonhomogeneous coverage of the bacteria and/or biomaterial surfaces by the cranberry derived PAC.

Careful inspection of the data presented in *Figure 4.3* reveals a greater absolute number of adhered cells for the *E. faecalis* versus the *E. coli*. For instance, for the control condition on PVC, there are 1×10^4 cells of *E. faecalis* attached per square cm, whereas there are 4×10^3 cells of *E. coli* attached per square cm. This result is in qualitative agreement with the predictions based on the steric Model. Specifically, the data summarized in *Table 4.2* shows energy barriers much larger in magnitude for the *E. coli* versus *the E. faecalis*. Furthermore, it is interesting to note that the model calculations predict greater energy barriers to deposition for attachment onto PVC in comparison to PTFE. Likewise, the results of the PPFC experiments reveal greater attachment to PTFE versus PVC. Finally, it can be noted in *Figure 4.3a* that the extent of *E. coli* attachment onto both PVC and PTFE is relatively comparable for all PAC treatments. Similarly, the predicted heights of the energy barrier are similar in magnitude for the three PAC treatments (*E. coli*) in comparison to the control condition.

There is increasing evidence in the literature pointing to the importance of secondary minimum deposition for bacteria and particle deposition onto inert surfaces. As not all deposition occurs within the primary energy minimum, secondary minima were examined with respect to adhesion data. This is particularily applicable in this application as energy barriers are in the order of 100,000 kT, a barrier far too high for deposition to occur in the primary energy minimum. The observed trend of adhesion (*Figure 4.3*) corresponds identically in all conditions with the depth of secondary energy minimum wells as predicted with the steric model (*Table 4.3*), with deeper wells associated with greater adhesion. Deposition in the secondary energy minimum is a weaker type of attachment that is evidenced by detachment during flow experiments. Kinetics data (*Figure 4.4)* compliments this evidence as latex adhesion and detachment was observed over the course of the experiment only under PAC supplemented conditions. The combination of experimental and theoretical evidence demonstrates that PAC inhibits adhesion through a mechanism of steric stabilization.

Table 4.3: Secondary minima from steric models of adhesion. *Secondary energy wells were calculated from the steric model (Eq. 2.1 + 2.14 + 2.19/20).*

	Treatment			
Bacteria-Biomaterial System	CTRL[a]	BAC	MAT	BOTH
E. coli-PVC				
depth of secondary minimum (kT)	-319	-294	-267	-98
h (nm) [b]	3.5	4.5	4.6	10
E. coli-PTFE				
depth of secondary minimum (kT)	-387	-293	-253	-89
h (nm)	2.7	4.5	4.6	10
E. faecalis-PVC				
depth of secondary minimum (kT)	-131	-112	-111	-41
h (nm)	3.6	4.6	4.6	10
E. faecalis-PTFE				
depth of secondary minimum (kT)	-183	-110	-107	-37
h (nm)	2.4	4.6	4.6	10

[a] For the control condition (i.e., no PAC), the XDLVO model was used for the interaction energy calculations.

[b] The separation distance (h) where the secondary energy minimum is located.

4.7 PAC Effects on Bacterial Protein Expression

Metabolic effects of cranberry juice on bacteria have been reported before in the literature ranging from changes in bacterial morphology [20] to inhibition of signaling molecules [26]. In this study it was found that even after a single generation of growth in media supplemented with PAC protein expression was altered. SDS-PAGE gel electrophoresis of *E. coli* CFTO73 whole protein (*Figure 4.7)* after a single culture grown in the presence of PAC (100 μg/mL), showed increased expression of a 20 kDa and 75 kDa proteins, with a 40 and 50 kDa protein conserved across all conditions.

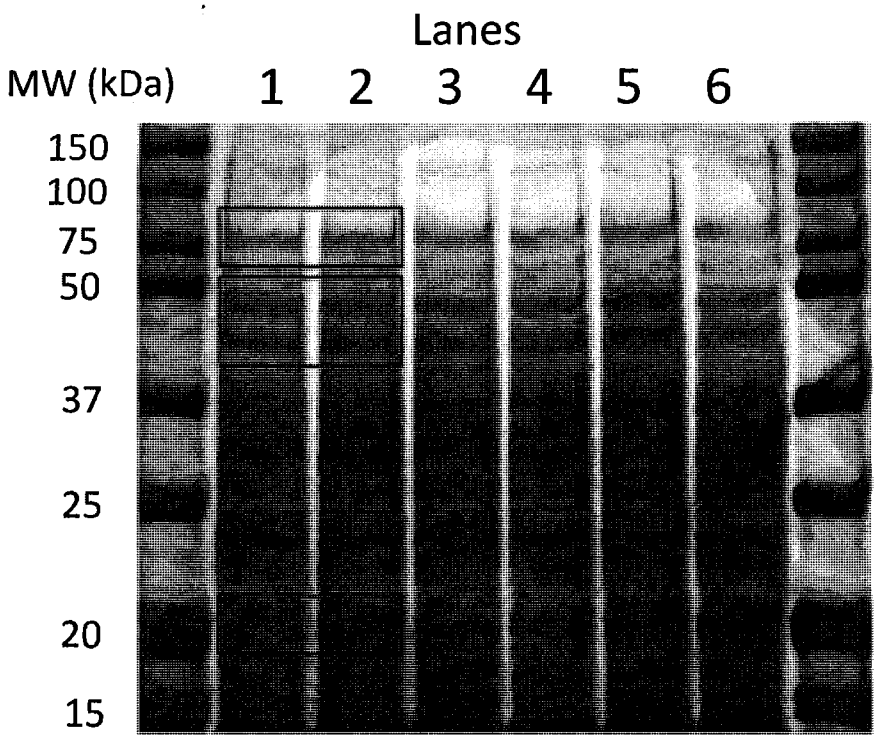

Figure 4.7: Effects of PAC on E. coli protein expression. *Whole cell lysate isolated from E. coli CFT073 grown with and without the presence of PAC was run on SDS-PAGE gels then silver stained and imaged. Lanes: (1) Molecular weight marker, (2) Control culture #1, (3) PAC culture #1, (4) Control culture #3, (5) PAC culture #3, (6) Control culture #6, (7) PAC culture #6, (8) Molecular weight marker. Increased expression of proteins near 20 kDa and 75 kDa suggest that some transcriptional processes are altered in bacteria exposed to PAC.*

In further pursuit of the identification of changes to transcriptional activity in the presence of PACs a DNA microarray is being pursued. It is of interest to further explore the nature of bacterial response to PAC in understanding both potential metabolic actions of PAC and further recognizing proteins responsible for bacterial adhesion.

Chapter Five
Conclusion

Catheter associated urinary tract infection is only one of many applications where the impact of any compound capable of preventing bacterial colonization hold an important impact. Other applications range in diversity from industrial piping and bioreactor construction to dentistry and skin-care.

Cranberry derived proanthocyanidins are effective in the inhibition of uropathogen adhesion to biomaterial surfaces as evidenced by the data in this thesis. Further this effect is mediated in part by steric interactions due to adsorption of the compound on both biomaterial and particle surfaces. There appear to be metabolic effects involved as well, the extent of which has yet to be determined. Importantly PAC acts in such a way that growth and viability of the microorganisms are not negatively altered, thereby reducing selective pressures for resistant bacteria.

The simplicity of the adsorption process to biomaterial surfaces makes the use of PAC in the treatment of medical devices significantly more feasible. The implementation of this natural system has the potential to decrease clinical financial expenditures related to catheter associated urinary tract infection and improve patient care. Further research is needed to explore the metabolic effect of PAC on microorganism, and drug delivery technologies, such as drug eluting biomaterial, in order to create a product that is safe, effective, and affordable.

Bibliography

1. Klevens, R., et al., *Estimating health care-associated infections and deaths in US hospitals, 2002.* Public Health Reports, 2007. **122**: p. 160-166.
2. Maki, D. and P. Tambyah, *Engineering out the risk for infection with urinary catheters.* Emerging Infectious Disease, 2001. 7(2): p. 342-7.
3. Trautner, B., R. Hull, and R. Darouiche, *Prevention of catheter-associated urinary tract infection.* Curr Opin Infect Dis, 2005. **18**: p. 37-41.
4. Donlan, R. and J. Costerton, *Biofilms: survival mechanisms of clinically relevant microorganisms.* Clinical Microbiology Reviews, 2002: p. 167-193.
5. Jepson, R., L. Mihaljevic, and J. Craig, *Cranberries for preventing urinary tract infections.* Cochrane Database Syst Rev, 2004. **2**(CD001321).
6. Foo, L., et al., *The structure of cranberry proanthocyanidins which inhibit adherence of uropathogenic P-fimbriated Escherichia coli in vitro.* Phytochemistry, 2000. **54**: p. 173-181.
7. Zafriri, D., et al., *Inhibitory activity of cranberry juice on adherence of type 1 and type p fimbriated escherichia coli to eucaryotic cells.* Anitmicrobial Agents and Chemotherapy, 1989. **33**(1): p. 92-98.
8. Saint, S., B.A. Lipsky, and S.D. Goold, *Indwelling Urinary Catheters: A One-Point Restraint?* Ann Intern Med, 2002. **137**(2): p. 125-127.
9. Trautner, B.W., R.A. Hull, and R.O. Darouiche, *Prevention of catheter-associated urinary tract infection.* Current Opinion in Infectious Diseases, 2005. **18**(1): p. 37-41.
10. Schembri, M.A., K. Kjaergaard, and P. Klemm, *Global gene expression in Escherichia coli biofilms.* Molecular Microbiology, 2003. **1**.
11. Costerton, J., et al., *The application of biofilm science to the study and contron of chronic bacterial infections.* Journal of Clinical Investigation, 2003. **10**(112): p. 1466-1477.

12. Gottenbos, B., H. van der Mei, and H. Busscher, *Models for studying initial adhesion and surface growth in biofilm formation on surfaces.* Methods Enzymol, 1999. **310**: p. 523-34.
13. Golomb, G. and A. Shpigelman, *Prevention of bacterial colonization on polyurethane in vitro by incorporated antibacterial agent.* Journal of Biomedical Materials Research, 1991. **25**(8): p. 937-952.
14. Christensen, G.D., et al., *Microbial and Foreign Body Factors in the Pathogenesis of Medical Device Infections*, in *Infections Associated with Indwelling Medical Devices*, A.L. Bisno and F.A. Waldvogel, Editors. 1989, American Society of Microbiology: Washington, DC. p. 27-59.
15. Van Oss, C.J., *Polar or Lewis Acid-Base Interactions*, in *Interfacial Forces in Aqueous Media*, C.J. Van Oss, Editor. 1994, Marcel Dekker: New York. p. 18-46.
16. Zhen, Q., P. Stoodley, and W. Pitt, *Effect of low-intensity ultrasound upon biofilm structure from confocal scanning laser microscopy.* Biomaterials, 1996. **17**(29): p. 1975-1980.
17. van der Borden, A., et al., *Electric current-induced detachment of Staphylococcus epidermidis biofilms from surgical stainless steel.* Applied and Environmental Microbiology, 2004. **70**(11): p. 6871-6874.
18. Xavier, J., C. Picioreanu, and S. Rani, *Biofilm-control strategies based on enzymic disruption of the extracellular polymeric substance matrix - a modelling study*

Microbiology, 2005: p. 3817-3832.
19. Dulawa, J., et al., *Tamm Horsfall glycoprotein interferes with bacterial adherence to human kidney cells.* Eur J Clin Invest, 1988. **18**(1): p. 87-91.
20. Ahuja, S., B. Kaack, and J. Roberts, *Loss of fimbrial adhesion with the addition of vaccinium macrocarpon to the growth medium of P-fimbriated Escherichia coli.* J Urol, 1998. **159**(2): p. 559-562.
21. Liu, Y.T., et al., *Role of cranberry juice on molecular-scale surface characteristics and adhesion behavior of Escherichia coli.* Biotechnology and Bioengineering, 2006. **93**(2): p. 297-305.
22. Greenberg, J.A., S.J. Newmann, and A.B. Howell, *Consumption of sweetened dried cranberries versus unsweetened raisins for inhibition of uropathogenic Escherichia coli adhesion in human urine: A pilot study.* Journal of Alternative and Complementary Medicine, 2005. **11**(5): p. 875-878.
23. Howell, A.B., et al., *Inhibition of the adherence of P-fimbriated Escherichia coli to uroepithelial-cell surfaces by proanthocyanidin extracts from cranberries.* New England Journal of Medicine, 1998. **339**(15): p. 1085-1086.
24. Hagerman, A.E. and L.G. Butler, *The specificity of proanthocyanidin-protein interactions.* The Journal of Biological Chemistry, 1981. **256**(9): p. 4494-4497.
25. Howell, A.B., et al., *A-type cranberry proanthocyanidins and uropathogenic bacterial anti-adhesion activity.* Phytochemistry, 2005. **66**(18): p. 2281-2291.
26. Camesano, T.A. in *232nd ACS Meeting.* 2006. San Francisco California.
27. Bailey, D.T., et al., *Can a concentrated cranberry extract prevent recurrent urinary tract infections in women? A pilot study.* Phytomedicine, 2007(14): p. 237-241.

28. Vorsa, N., et al., *Structure and genetic variation of cranberry proanthocyanidins that inhibit adherence of uropathogenic P-fimbriated E-coli*, in *Food Factors in Health Promotion and Disease Prevention*. 2003. p. 298-311.
29. Ohnishi, R., et al., *Urinary excretion of anthocyanins in humans after cranberry juice ingestion.* Bioscience Biotechnology and Biochemistry, 2006. **70**(7): p. 1681-1687.
30. Wilson, W., et al., *Status of methods for assessing bacterial cell surface charge properties based on zeta potential measurements.* J. Microbiol. Methods, 2001. **43**: p. 153-164.
31. Peterson, A., R. Hancock, and E. McGroarty, *Binding of polycationic antibiotics and polyamines to lipopolysaccharides of Pseudomonas aeruginosa.* J Bacteriology, 1985(164): p. 1256-1261.
32. Makin, S. and T. Beveridge, *The influence of A-band and B-band lipopolysaccharide on the surface characteristics and adhesion of Pseudomonas aeruginosa to surfaces.* Microbiology, 1996. **142**: p. 299-307.
33. Sokurenko, E.V., et al., *Functional heterogeneity of Type-1 fimbriae of Escherichia coli.* Infection and Immunity, 1992. **60**(11): p. 4709-4719.
34. Danese, P.N., et al., *The outer membrane protein, antigen 43, mediates cell-to-cell interactions within Escherichia coli biofilms.* Molecular Microbiology, 2000. **37**(2): p. 424-432.
35. Klemm, P., et al., *Structure-function analysis of the self-recognizing Antigen 43 autotransporter protein from Escherichia coli.* Molecular Microbiology, 2004. **51**(1): p. 283-296.
36. Kjaergaard, K., et al., *Antigen 43 facilitates formation of multispecies biofilms.* Environmental Microbiology, 2000. **2**(6): p. 695-702.
37. Roche, A.J., J.P. McFadden, and P. Owen, *Antigen 43, the major phase-variable protein of the Escherichia coli outer membrane, can exist as a family of proteins encoded by multiple alleles.* Microbiology, 2001. **147**(1): p. 161-169.
38. van Oss, C., *Interfacial forces in aqueous media.* 1994, New York: Marcel Dekker, Inc.
39. Elimelech, M., et al., *Particle Deposition & Aggregation.* Colloids and Surface Engineering Series, ed. R. Williams. 1998: Butterworth-Heinemann.
40. Gregory, J., *Approximate expression for retarded van der Waals interaction.* J Coll Interf Sci, 1981. **83**: p. 138-145.
41. Hogg, R., T. Healy, and D. Fuerstenau, *Mutual coagulation of colloidal dispersions.* Trans Faraday Soc, 1966. **62**: p. 1638-1651.
42. Roosjen, A., et al., *Bacterial factors influencing adhesion of Pseudomonas aeruginosa strains to a poly(ethylene oxide) brush.* Microbiology, 2006. **152**: p. 2673-2682.
43. de Gennes, P., *Polymers at an interface; a simplified view.* Advances in Colloid and Interface Science, 1987. **27**(3-4): p. 189-209.
44. Anfort, A., et al., *Roles of serine accumulation and catabolism in the colonization of the murine urinary tract by Escherichia coli CFT073.* Infect Immun, 2007. **75**(11): p. 5298-304.
45. Hiemenz, P., *Principles of Colloid and Surface Chemistry*, ed. L. Lagowski. 1992, New York & Basel: Marcel Dekker.

46. Van der Mei, H., R. Vos, and H. Busscher, *A reference guide to microbial cell surface hydrophobicity based on contact angles.* Coll Surf B, 1998. **11**: p. 213-221.
47. Walker, S., et al., *A novel asymmetric clamping cell for measuring streaming potential of flat surfaces.* Langmuir, 1999. **6**: p. 2193-2198.
48. Derjaguin, B. and L. Landau, *Theory of the stability of strongly charge lyophobic sols and of the adhesion of strongly charged particles in solutions of electrolytes.* Acta Physicochim URSS, 1941. **14**: p. 733-762.
49. Verwey, E. and J. Overbeek, *Theory of the stability of lyophobic colloids*. 1948, Amsterdam: Elsevier.
50. Rijnaarts, H., et al., *DLVO and steric contributions to bacterial deposition in media of different ionic strengths.* Colloids and Surfaces B, 1999. **14**: p. 179-195.
51. Woodle, M. and D. Lasic, *Sterically stabilized liposomes.* Biochimica et Biophysica Acta, 1992. **1113**: p. 171-199.
52. Napper, D., *Steric stabilization.* J Coll Interf Sci, 1977. **58**(2): p. 3315-3331.
53. Azeredo, J., J. Visser, and R. Oliveira, *Exopolymers in bacterial adhesion: interpretation in terms of DLVO and xDLVO theories.* Coll Surf B, 1999. **14**: p. 141-148.
54. Kuznar, Z. and M. Elimelech, *Direct microscopic observation of particle depositionin porous media: Rol of secondary energy minimum.* Coll Surf A, 2007. **294**: p. 156-162.
55. Hahn, M., D. Abadzic, and C. O'Melia, *Aquasols: On the Role of Secondary Minima.* Environ Sci Technol, 2004. **38**: p. 5915-5924.
56. Litton, G. and T. Olson, *Particle size effects on colloid deposition kinetics: evidence of secondary minimum deposition.* Coll Surf A, 1996. **107**: p. 273-283.

Appendix